

# **Thermal Analysis in Hiemenz Flow of Viscous Fluid with Hybrid Nanoparticles**

**By**  
**Nadia Khurshid**



**NATIONAL UNIVERSITY OF MODERN  
LANGUAGES ISLAMABAD**

**March, 2024**

# **Thermal Analysis in Hiemenz Flow of Viscous Fluid with Hybrid Nanoparticles**

**By**

**Nadia Khurshid**

MS Mathematics, National University of Modern Languages, Islamabad, 2024

A THESIS SUBMITTED IN PARTIAL FULFILMENT  
OF THE REQUIREMENTS FOR THE DEGREE OF

**MASTER OF SCIENCE**

**Mathematics**

To

FACULTY OF ENGINEERING & COMPUTING



NATIONAL UNIVERSITY OF MODERN LANGUAGES ISLAMABAD

© Nadia Khurshid, 2024



## THESIS AND DEFENSE APPROVAL FORM

The undersigned certify that they have read the following thesis, examined the defense, are satisfied with overall exam performance, and recommend the thesis to the Faculty of Engineering and Computing for acceptance.

**Thesis Title:** Thermal Analysis in Hiemenz Flow of Viscous Fluid with Hybrid Nanoparticles

**Submitted By:** Nadia Khurshid

**Registration #:** 15 MS/MATH/F20

Master of Science in Mathematics

Title of the Degree

Mathematics

Name of Discipline

Dr. Awais Ahmed

Name of Research Supervisor

Signature of Research Supervisor

Dr. Sadia Riaz

Name of HOD (MATH)

Signature of HOD (MATH)

Dr. Muhammad Noman Malik

Name of Dean (FEC)

Signature of Dean (FEC)

March, 2024

# AUTHOR'S DECLARATION

I Nadia Khurshid

Daughter of Muhammad Khurshid

Registration # 15 MS/Math/F20

Discipline Mathematics

Candidate of **Master of Science in Mathematics (MS Math)** at the National University of Modern Languages do hereby declare that the thesis "**Thermal Analysis in Hiemenz Flow of Viscous Fluid with Hybrid Nanoparticles**" submitted by me in partial fulfillment of MS\_Math degree, is result of my own research except as cited in references. This thesis has not been submitted or published earlier. I also solemnly declare that it shall not, in the future, be submitted by me for getting any other degree from this or any other university or institution. I also understand that if evidence of plagiarism is found in my thesis at any stage, even after the award of a degree, the work may be canceled and the degree revoked.

---

Signature of Candidate

Nadia Khurshid

Name of Candidate

March, 2024

Date

## **ABSTRACT**

### **Title: Thermal Analysis in Hiemenz Flow of Viscous Fluid with Hybrid Nanoparticles**

As opposed to conventional nanofluids, hybrid nanofluids are regarded as more suited fluids in practical applications of heat transfer. Since the hybrid nanofluids' combined properties of two or more nanomaterials result in greater thermal conductivity of base liquid. The present study examines heat transfer in a Hiemenz flow over bi-directionally stretched sheets by comprising hybrid nanoparticles (SWCNT, MWCNT with base fluid water). Additionally, the heat transfer phenomenon is analyzed in the presence of magnetic field effect. The partial differential equations are subjected to the appropriate similarity transformations in order to create a dimensionless system of equations. A dimensionless system using the bvp4c approach (MATLAB-builtin function) is solved numerically and outcomes presented in graphical forms. Effects of the dimensionless physical parameters on flow and thermal profile is also discussed. By comparing basefluid, nanofluid (SWCNT and water), and hybrid nanofluid (SWCNT, MWCNT and water), the effects of dimensionless parameters on velocity and temperature are graphically abstracted. Physical explanation effectively support the study's findings.

# TABLE OF CONTENT

CHAPTER	TITLE	PAGE
	TABLE OF CONTENTS	iv
	LIST OF FIGURES	vii
	LIST OF TABLES	ix
	LIST OF SYMBOLS	x
	ACKNOWLEDGEMENT	Xii
1	INTRODUCTION	1
2	LITERATURE REVIEW	7
	2.1 Research Objectives	24
	2.2 Significance of the study	25
3	PRELIMINARIES	26
	3.1 Basic Definitions and formulas	26
	3.1.1 Fluid	26
	3.1.2 Fluid mechanics	26
	3.1.3 Fluid statics	26
	3.1.4 Fluid dynamics	26
	3.1.5 Density	27
	3.1.6 Pressure	27
	3.1.7 Stress	27
	3.1.8 Shear stress	27
	3.1.9 Normal stress	27
	3.1.10 Strain	28
	3.1.11 Viscosity	28
	3.1.12 Dynamic viscosity	28
	3.1.13 Kinematic viscosity	28
	3.1.14 Newton's law of viscosity	28
	3.1.15 Newtonian fluids	29

3.1.16	Non-Newtonian fluids	29
3.1.17	Flow	29
3.1.18	Incompressible flow	29
3.1.19	Compressible flow	29
3.1.20	Laminar flow	30
3.1.21	Turbulent flow	30
3.1.22	Steady flow	30
3.1.23	Unsteady flow	30
3.1.24	Viscous Nanofluid	30
3.1.25	Hybrid Nanofluid	31
3.1.26	Stagnation Point	31
3.1.27	Stagnation point flow	31
3.1.28	Thermal Conductivity	32
3.1.29	Thermal diffusivity	32
3.1.30	Modes of heat transfer	33
3.1.31	Viscous Dissipation	33
3.1.32	Magnatohydrodynamic (MHD)	33
3.1.33	Heat generation/absorption	34
3.1.34	Lorentz force	34
3.1.35	Fouier's law	34
3.1.36	Brownian motion	34
3.1.37	Buoyancy force	35
3.2	Dimensionless numbers	35
3.2.1	Reynolds number	35
3.2.2	Lewis number	35
3.2.3	Prandtl number	36
3.2.4	Eckert number	36
3.2.5	Nusselt number	37
3.2.6	Skin friction	37
3.2.7	Conservation laws	38

<b>4</b>	<b>Hiemenz stagnation-point flow with heat transport over bi-directional stretching sheet under magnetic field</b>	<b>39</b>
4.1	Introduction	39
4.2	Mathematical Formulation	39
4.3	Numerical Problem	42
4.4	Discussion of result	43
<b>5</b>	<b>Flow of hybrid nanofluid in Hiemenz's theory over stretchable Surface</b>	<b>53</b>
5.1	Introduction	53
5.2	Mathematical formulation	53
5.3	Numerical solution	56
5.4	Presentation result	58
<b>6</b>	<b>Conclusions</b>	<b>67</b>
<b>7</b>	<b>Future work</b>	<b>67</b>
<b>8</b>	<b>References</b>	<b>68</b>



## LIST OF FIGURES

FIGURE NO.	TITLE	PAGE
3.1	Hybrid Nanofluid	31
3.2	Stagnation Point	32
4.1	Flow Diagram	40
4.2	(a-c): Impact of $M$ on flow field (stretching)	46
4.3	(a,b): Impact of $M$ on flow field (Shrinking)	47
4.4	(a-c): Impact of $\beta$ on flow field (Stretching)	48
4.5	(a,b): Impact of $\beta$ on flow field (Shirinking)	49
4.6	(a,b): Impact of $\alpha$ on temperature and concentration field	50
4.7	(a,b): Impact of $N_t$ and $N_b$ on temperature and concentration Field	51
4.8	(a,b): Impact of $\alpha$ and $M$ on stress parameters $\{f''(0), g''(0)\}$	52
5.1	Geometry of the problem	54
5.2	Influence of $M$ (stretching) on velocity profile	59
5.3	Influence of $M$ (shrinking) on velocity field	60
5.4	Influence of $a_1$ (stretching) on velocity profile	60
5.5	Influence of $a_1$ (shrinking) on velocity profile	61
5.6	Influence of $b_1$ (stretching) on velocity profile	61
5.7	Influence of $b_1$ ( shrinking) on velocity field	62
5.8	Influence of $M$ (stretching) on velocity field	62
5.9	Influence of $a_1$ (stretching) on velocity field	63
5.10	Influence of $b_1$ (stretching) on velocity filed	63
5.11	Influence of $M$ (stretching) on temperature profile	64
5.12	Influence of $M$ (shrinking) on temperature profile	64
5.13	Influence of $b_1$ (shrinking) on temperature profile	65
5.14	Influence of $a_1$ (stretching) on temperature profile	65

5.15	Influence of $\alpha_1$ (shrinking) on temperature	66
5.16	Influence of Pr on temperature profile	66

## LIST OF TABLES

<b>TABLE NO.</b>	<b>TITLE</b>	<b>PAGE</b>
5.1	The thermophysical characteristics of the analysed nanofluid	57
5.2	Thermophysical characteristics for the hybrid nanofluids	57
5.3	Thermophysical characteristics of base fluid (water) and Nanoparticles	58

## LIST OF SYMBOLS

$x, y$	-	Cartesian coordinates
$u, v$	-	Components of velocity
$M$	-	Magnetic Field
$\mu_f$	-	Dynamic viscosity
$\nu_f$	-	Kinematic viscosity
$\rho_f$	-	Density
CNTs	-	Carbon nanotubes
SWCNT	-	Single wall Carbon nanotubes
MWCNT	-	Multi wall Carbon nanotubes
MHD	-	Megnatohydrodynamic
$Ec$	-	Eckert number
$N_t$	-	Thermophoresis parameter
$K_f$	-	Thermal conductivity
$Cf_x$	-	Skin fraction coefficient
$N_b$	-	Brownian diffusion coefficient
$T_m$	-	Surface temperature
$U_w$	-	Stretching velocity
$\frac{d}{dt}$	-	Material derivative
$T_\infty$	-	Free Stream Temperature
$(C_p)_f$	-	Specific heat capacity
$Le$	-	Lewis Number
$\Phi_1$	-	SWCNT volume friction
$\Phi_2$	-	MWCNT volume friction
$K_{swcn}$	-	Thermal conductivity of SWCNTs
$\theta$	-	Non-dimensional temperature
$f'$	-	Non-dimensional velocity
$Sh_x$	-	Sherwood Numbers

$C_{\infty}$	-	Free stream concentration
Re	-	Reynolds Number
Pr	-	Prandtl Number
$Nux$	-	Nusselt number
T	-	Temperature

## **ACKNOWLEDGEMENT**

Firstly, In the name of Almighty Allah, the most Merciful and Compassionate, All the worship and honor is for Him, Who always helped me to stick to the right path and always provided me the courage and strength to complete my degree with hard work and dedication.

I would like to convey my heartfelt thanks and admiration to Dr. Awais Ahmed, my highly esteemed supervisor. Throughout my academic journey, he provided me with invaluable aid and inspiration to ensure the timely completion of all tasks assigned to me. His constant support and expertise helped me successfully navigate every aspect of writing my thesis. As a result, I will always cherish his selfless contributions and keep him in my prayers.

I want to express my gratitude to the Department of Mathematics, National University of Modern Languages, Islamabad for providing me with a diverse range of learning methods through their dedicated staff and faculty members.

My gratitude goes out to my parents and siblings, whose aid, motivation, and unwavering backing have been invaluable. Their unwavering assistance has been my backbone as their prayers have kept me going up to this point.

Nadia Khurshid

## DEDICATION

*My family and supervisor have played a crucial role in my dissertation work. I'm especially grateful to my parents, who instilled in me the values of working hard with dignity and humility and never giving up on hope and faith. Equally important has been my Supervisor, who serves as a true mentor for me, and continues to inspire, uplift, and provide guidance so I can complete my research within the designated timeframe.*

# CHAPTER 1

## INTRODUCTION

Fluid dynamics is a subfield of continuum science that studies how fluids move, whether they follow Newtonian or non-Newtonian laws. Because of its adaptable traits, it is widely used in both the natural sciences and engineering sectors and has a wide range of applications in engineering mechanisms. In recent years, nanofluids have received a lot of interest due to their wide availability in manufacturing industries like paper, the pharmaceutical business, and the medical industry, among others. Nanofluids consist of basic fluids (oils, lubricants, & ethylene glycol are examples along with polymeric solutions, biologic fluids, etc.) including nanoparticle (metals, oxides, carbide, etc.) with a typical size of less than 100 nm. These are fluid solutions of nanoparticles used to improve the thermophysical properties of base fluids and to improve the heat transfer characteristics since particles that are solid have a higher thermal conductivity than liquids. Choi first used the term "nanofluids" in 1995. According to Choi, base fluids are not comparable to the thermal conductivity of nanofluids. Turcu (2006) & Jana (2007) modified the 1995 discovery of nanofluids by developing the groundwork for hybrid nanofluids. The promising results of nanofluids led scientists to think about dispersing different nanoparticle arrangements within a base fluid.

'Hybrid nanofluids' are an interesting category of fluids that were created as a result of the expansion of nanofluids. In comparison to nanofluids having only one kind of nanoparticle, a hybrid nanofluid with higher thermal conductivity is produced when more than one kind of nanoparticles are carried in a base fluid. In addition to numerous other uses, hybrid nanofluids have been studied for use in collectors for solar photovoltaic thermal processing, electronic component heat management, engine applications, and vehicle cooling.

Liu *et al.* [1] carried out an experimental investigation to improve thermal energy conduction in a base fluids like water. The Cu nanoparticles utilize in this work were produced using a chemical reduction technique. Sharma *et al.* [2] proved that in their investigation the concentration of different solid nanoparticles increase the thermal conduction of conventional



fluid. *Huang et al.* [5] proposed the use of nanotubes made of carbon as a nanoparticles in the base fluid in a chevron corrugated-plate exchanger for heat transfer. *Albeshri et al.* [9] numerically examined the hydrodynamic study of a laminar forced convective hybrid nanofluid (Ag-TiO<sub>2</sub>/water) flow at the opening region of a horizontal annulus, with uniform heat flux situation and adiabatic at outer and inner wall, respectively. Some of the recent studies on the thermal and hydrodynamics characteristics of hybrid nanofluid can be seen here (see Refs. [10-14]). *Reddy et al.* [17] a sliding vertical plate along porosity was used to demonstrate the instability of magnetohydrodynamic convection flow. *Haritha et al.* [20] in the presence of a magnetic field, temperature, heat source, and chemical reaction, the combined effects of Navier slip plus flow boundary conditions on an unsteady flow of an MHD flow across a stretching sheet are examined.

*Ahmad et al.* [23] demonstrate the influence of Joule heating and three-dimensional magneto hydrodynamic Maxwell nanofluids on a thin stretched surface. The impacts of binary chemical reactions, heat production, heat flow, and the thermophoretic effects are all taken into consideration. The various slip condition requirements are applied at the surface's edge. It can be demonstrated that fluid velocities are lowered by the magnetic, fluid relaxation, as well as thickness of walls properties. The velocity, density, as well as temperature slip factors also lower the fluid's temperature, flow rate, and densities distribution. *Wahid et al.* [26] his research primarily focuses on radiation flow of a hybrid aluminium oxide nanofluid through a porous plate containing mixed convection at the MHD stagnation point. In this work, he consider that the hybridized of both sorts of nanoparticles, notably copper and alumina, in contrast to the traditional nanofluid model, which only considers one type of nanoparticles. The presence of opposing flow brought on by the combination of convection and radiation factors can improve heat transfer when the copper concentration volume is decreased and the radiative and magnet parameters are multiplied. According to *Waqas et al.* [30] work, thermal radiation is relevant when a nanofluid is flowing across a stanching surface and serves as a heat source and sink. Here, an ethylene glycol base fluid is infused with nanoparticles of copper, aluminium oxide, and oxide of graphite. His analysis' findings show that the fluid velocity increases with greater Deborah number changes while decreasing with increasing estimations of the magnetic parameter. In contrast to rising Deborah number variations, the thermal distribution profile showed decreasing results for increasing Biot number and heat transfer variations. *Gangadhar et al.* [33] examined Hybrid nanofluid may be regarded as a different form of nanofluid because of its thermal characteristics and potential use in heat

exchange studies. The major objective of this study is to establish a connection between traditional and hybrid nanofluid qualities based on viscous incompressible, micropolar theory, and the the conclusion of thermal energy is heating a surface that has been stretched exponentially. Comparisons of the properties of blood that is noble, MgO/blood the nanofluid and Au-MgO/blood hybrid nanofluid are possible by displaying the velocity, microrotation, as well as temperature field graphs. For a more thorough knowledge from the heat and fluid flow rate of a gearbox within a nanofluid + hybrid nanofluid, the results of the coefficient of friction and Nusselt value are also provided. The analysis's concluding findings include the fact that even when micropolar effects, convection conditions and viscous dissipation are present, hybrid nanofluid heat exchange rates are 13.8 percentage higher than that nanofluid. Lastly, platelet-sized particles transmit heat more quickly than other nanoparticles.

*Seddeket et al.* [39] the relationship between radiation and thermal diffusion and heat transmission across a stretching surface with variable heat flux has been studied. The relationship between the heat flux and temperature is thought to be linear. The correct analytical answer for such velocity is given, as well as a mathematical model for such a temperature field. Numerical solutions are provided for various values of variable heat transfer, radiation, Prandtl number and temperature parameter. *Qi et al.* [41] highlight the most current improvements in hybrid nanoparticle miniemulsion synthesis since 2009. These hybrid nanoparticles are polymeric, polymeric-natural macromolecule hybrids, and hybrid organic-inorganic nanoparticles. They can be made through transplanting polymerization throughout, from, or through natural macro molecules. They can also be made through solvent displacement techniques, miniemulsion (co)polymerization, simultaneous polymerise of polymers produced from vinyl and vinyl-containing inorganic predecessors, precipitation of preformed polymer compounds in the presence of inorganic elements, and solvent displacement are all examples of polymerization processes. The properties, qualities, and applications of hybrid nanoparticles are also explored. *Aaron et al.* [42] described that a new optical imaging technique that combines the benefits of magnetic actuation and molecularly driven plasmonic nanoparticles. Hybrid nanoparticles with a gold coating and an iron oxide core are used to create this mixture. The development component epidermal receptors, a widely used cancer biomarker, is the target of the infrared signal from the nanoparticles, while the gold's element resonantly scattered light that is visible to create a potent optical signal. Strong plasma resonance (PR) scattering and magnetic actuation greatly boost the contrast in photographs of cells that have been marked with hybrid gold/iron nanoparticles of oxide.

*Devarajan et al.* [43] his work discuss the thermophysical properties of the applications for CNT/Al<sub>2</sub>O<sub>3</sub> hybrid nanofluids in heat transmission. CNT and Al<sub>2</sub>O<sub>3</sub> nanoparticles were introduced to the starting fluid in equal amounts for two different concentrations of 0.05 and 0.1%. The outcomes demonstrate that the thermophysical properties of nanotube nanofluid are improved by adding a handful of Al<sub>2</sub>O<sub>3</sub> nanoparticles. At the final concentration is 0.1%, the hybrid nanofluids enhanced by 20%, although the heat conductivity of CNT itself rose by just eight percent at the base fluid. Similar to this, hybrid nanofluid's viscosity and density have increased by up to 10% as well as 7%, respectively, in comparison to base fluid. At the final concentration of 0.2%, the hybrid nanofluids' specific thermal energy capacity rises to roughly 138% that of CNT nanofluid.

*Nalivela et al.* [47] explain a stretching surface is used in MHD spontaneous convection to transfer mass from an impermeable, viscous fluid, and the effects of radiation and viscosity dissipation are investigated. Investigated and visually illustrated is the impact of non-dimensional parameters on concentration, temperature, temperature and velocity. It has been discovered that the temperature profiles grow as the influence of the chemical variable, Eckert number, radiation, Schmidt number and the magnetic parameter (M) increases, while the velocity profile falls as these parameters increase. Additionally examined and compiled in tabular form for different quantities of the chemical procedure, magnetic field, and Schmidt number are the friction factor, Nusselt, and Sherwood numbers. The findings of this research received considerable support from modern scholarship. *Aly et al.* [51] highlight the continuous stagnation point flows and heat transmission across a stretching/shrinking surfaces were theoretically and numerically explored in a hybrid nanofluid containing partial sliding and viscous dissipation. It was discovered that the hybrid nanofluid works better as a heater while the magnetic parameter is increased but works better as a cooler when the Eckert number, slip parameters stretching are all increased. For shrinking sheets, critical zones of single or dual solutions have been proposed. While examining the unique/dual solution's consistency, three zones of stabilisation were found. It was determined that the velocity and elevation are substantially more easily accessible closer to the terminated line in the dual solution area. It has also been proven that they act in each of the three stability zones in a completely in a distinct manner. *Labib et al.* [55] explained the examination of forced convection transfer of heat of the nanofluid using a mixture with two phase's model yields a novel notion for improving heat transfer. Two different base fluids are employed separately to find out how

base fluids impact convective thermal blending of  $\text{Al}_2\text{O}_3$  nanoparticles. The computational technique has been successfully verified with the experimental information that has been published in the literature in the case of  $\text{Al}_2\text{O}_3$ /water nanofluids. According to the results, water does not improve heat transmission as well as ethylene glycol when used as the base fluid.  $\text{Al}_2\text{O}_3$  nanoparticles, CNTs, and water are combined. The term "nanofluids" relates to a cutting-edge concept of hybrid or combined nanofluids that can significantly increase convective heat transmission.

*Nabwey et al.* [58] an extensive study of him is In a stretched sheet under forced heat flux (PHF) and surface temperature (PST) circumstances, magnetohydrodynamics flow occurs via the boundary layer of an a non-New micropolar the nanofluid with hybrid characteristics ( $\text{Fe}_3\text{O}_4$  -Ag) immersed with transmitting micrometre evenly sized dust nanoparticles. Thermal relaxation increases at the micropolar the nanofluid hybrid and particle stages, which strengthen temperature fluctuation. *Jana et al.* [62] explained that numerous nanomaterials' naturally high thermal conductivity has the potential to greatly enhance applications involving the fluidic transmission of heat.

In this study, conductive nanoparticles like carbon nanotubes (CNTs), gold nanoparticles (AuNPs), copper nanoparticles (CuNPs), and hybrids of these materials like CNT-CuNP or CNT-AuNP were employed to improve fluid heat transfer. The increase in heat conductivity that was seen in mono-type nanoparticle solutions and was aided by the use of CuNPs was the biggest. However, hybrid suspensions weren't developing to the same degree. The measured thermal conductivities of a number of nanofluids consistently surpassed the predictions generated by previous mathematical models. The mechanisms enhancing thermal conductivity are the subject of discussion. It was discovered that the degree of stability was influenced by the characteristics of the nanoparticles through measuring nanofluid stability using a UV-vis-NIR spectrophotometer.

*Roy et al.* [64] highlight on the transfer of mass and heat of a nanofluid hybrid that flow across a permeable stretched surface, the results of a binary chemical response controlled by activation energy were examined. Two solutions appeared within a predetermined time interval when the sucking parameter was fixed. The results show that as the presence of two solutions increases, the amount and percentage of copper nanoparticles, the Richardson's number, and the total buoyancy forces parameter rise as well. The diverse concept is seen as the stretching

variable, temperature difference variable, and aluminum nanoparticle volume fraction improve Local Nusselt number, friction in the skin coefficients, and Sherwood number all enhance as a function of the volume of copper nanoparticles, the suction parameter, Richardson's number, and linked forces of buoyancy parameters. For the mass transfer, only a small amount of the without dimensions energy of activation is needed, which gets more pronounced as the fitted rate stable, non-dimensional reaction rate temperature differential parameter rise. The flow properties are significantly affected by changes in the stretching parameter, suction parameter, and nanoparticle volume fraction. *Abu Bakar et al.* [70] this study looks at how a hybrid nanofluid moves through a porous, permeable Darcy medium with slip, radiation, shrinking sheet, and radiation characteristics. Hybrid nanofluid including its thermophysical characteristics have been studied since the turn of the millennium.  $\text{Al}_2\text{O}_3$ -Cu/water functions as the second fluid in this case, with Cu/water represents a base nanofluids. It is discovered that the non-uniqueness of solution occurs over the range that encompasses the shrinking parameter, making it difficult to identify a larger solution than one that exists across the upper and lower branches. The investigation indicates that the hybrid nanofluid transfers heat more quickly than the normal nanofluid.

## CHAPTER 2

### LITERATURE REVIEW

The hybrid nanofluids, a different type of nanofluids, have a wide range of industrial uses. For instance, using hybrid nanofluid instead of fins to improve the efficiency of a heat exchanger, or using nanofluid as a coolant in numerous different heat transfer devices. The transport of heat energy is a crucial mechanism in many commercial processes since it significantly affects the quality of the final product. When processing polymers, for instance, predicting the temperature profile is essential for melting and solidification. Researchers are focusing on improving thermal energy transfer in buoyancy forces liquids with limited heat conductivity and studying thermal analysis. Due to the use of these new innovative liquids, there is no need to any structural changing in the heat exchanger.

*Liu et al.* [1] performed the experimental study for the improved conduction of thermal energy in base fluid as water. In this study, the Cu nanoparticles have been generated to use a chemical reduction method. *Sharma et al.* [2] proved that in their investigation the concentration of different solid nanoparticles enhances the thermal conduction of conventional fluid. The use of copper-titanium/water hybrid nanofluid as coolant in heat exchanger was explored by *Madhesh and Kalaiselvam* [3] in the experimental study. The different volume fraction was considered to explore the forced convection characteristics. The results proved that the convection coefficient reach its maximum range for 0.7% of particle concentration the base fluid. Thermal enhancement in the 3D flow hybrid nanofluid influenced by heat source and thermal radiation was proved by *Hayat and Nadeem et al.* [4].

In a chevron corrugated-plate heat exchanger the idea for the use of Carbon nanotubes as a nanoparticle in the base fluid was given by *Huang et al.* [5]. They establish the correlation for thermal energy transfer in the heat exchanger. Convective stagnation point flow of hybrid nanofluid both naturally and artificially was explored by *Rostami et al.* [6] through multiple solutions. Forced and free convection phenomena in the flow of hybrid nanofluid over riga

plate was investigated numerically by *Khashi'ie et al.* [7]. The phenomenon of naturally and artificially convective flow in a trapezoidal cavity contains hybrid nanofluid (Cu-Al<sub>2</sub>O<sub>3</sub>/water) was examined by *Cimpean et al.* [8] through the numerical findings. Hydrodynamic analysis of a laminar forced convective hybrid nanofluid (Ag-TiO<sub>2</sub>/water) flow in the opening region of a horizontal annulus was investigated by *Albeshri et al.* [9] numerically, with uniform heat flux condition and adiabatic at outer and inner wall, respectively. Some of the recent studies on the thermal and hydrodynamics characteristics of hybrid nanofluid can be seen here (see Refs. [10-14]).

Natural convective stagnation point flow over a horizontal and vertical boundary such as sheet, cylinder, cone and disk practically very important because a lot of applications can be found in the industry for this problem. Most of the cooling process at large scale encountered this type of flow phenomenon. A vertically heated flat surface immersed in water was explored by *Haq et al.* [15] for natural convective fluid motion through the medium with porosity and magnetic field. The findings of the study showed that under mixed convection, the velocity profile exhibits rising behavior for varied values of the power index  $m$ . The thermal analysis in free convective flow of nanofluid passing through porous medium was provided by *Oyelakin et al.* [16]. The viscosity, thermal conductivity, and Brownian diffusion of nanofluids was considered as concentration dependent. When thermal radiation and consistent chemical reaction are present, *Reddy et al.* [17] presented the unsteady magneto hydrodynamic natural convective flow of a double diffusive fluid over a moving vertical plate with porosity. Sinusoidal fluctuations surface temperature impact on the free convection flow of ferrofluid across a heated sheet was examined by *El-Zahar et al.* [18]. A numerical approach known as the hybrid linearization-differential quadrature technique is used to solve the governing equations of the physical problem. The free convective flow of a rotating upright cone above a time-independent hybrid nanofluid was studied in a permeable medium by *Tlili et al.* [19]. Additionally, leftover Engine Oil (EO) was used to scatter the nanoparticles of TC4 (Ti-6Al-4V) as well as Nichrome, also (80% Ni, 20% Cr).

*Haritha et al.* [20] On an unsteady flow of a Mhd flow across a stretching sheet in the presence of a magnetic field, thermal, heat source, and chemical reaction, the combined effects of Navier slip and flow boundary conditions are analyzed. *Madhu et al.* [21] it is thought about how the stretching of a sheet with thermal radiation may affect non-Newtonian Maxwell the nanofluid boundary layer flow. The electromagnetic concept is still utilised to explain the behaviour of non-Newtonian fluids. The flow properties, heat transmission characteristics, and

the volume percentage of nanoparticles are all carefully considered and reported for different combinations of the governing flow parameters. *Alsaedi et al.* [22] conducted a numerical study of the flow of a nanofluid over two coaxially constructed cylinders. The nanomaterial is composed of graphene oxide (GO) and copper (Cu) nanoparticles in kerosene oil basefluid. This mixed nanofluid fills these two coaxial cylinders. The inner cylinder does not move, while the outer cylinder does. Using an incessant magnetic field in the radial direction, the characteristics of heat transfer and flow are investigated. Joule heating is also taken into account. Higher magnetic parameters result in a decrease in velocity for both the nanofluid composed of a hybrid (GO + Cu/Kerosene oil) as the pure Cu/Kerosene oil nanofluid. In contrast to increasing nanoparticle concentration fraction for copper, a temperature decline is observed.

*Ahmad et al.* [23] examined a thin stretched surface with a three- dimensional magneto hydrodynamic Maxwell nanofluids and Joule heating. Further taken into account are the effects of binary chemical processes, heat production, heat flux, and the thermophoretic effect. At the surface's boundary, the multiple slip condition conditions are used. It can be shown that the magnetic, fluid relaxation and wall thickness properties reduce fluid velocities. Furthermore, the fluid's velocity, temperature, and density distribution are reduced by the velocity, density, and temperature slip parameters. *Acharya et al.* [24] explains that many industrial and technological applications, including semiconductors, turbines, electric transformers, vehicle radiators, heat transfer, fuel cells made of hydrogen, air-cooled engines, etc. utilize various geometrical shapes of fins. Nanofluids investigate better thermal conductivities in comparison to traditional coolants, promoting exceptional heat transport abilities. The research of both the thermal fallouts of naturally convective laminar magnetic induced Aerospace hybrid nanofluid flows inside a circular enclosures fitted with I-shaped square fins of various lengths is motivated by such exceptional remarkable applications. *Neethu et al.* [25] investigated microorganisms improve the fluid's stability, which is important for microbiology, micro, and micro coolant systems. The behavior of evolvable MHD nanofluids containing ( $\text{TiO}_2$  and Ag in water) movement across an exponentially expanding permeable surface has thus been studied while taking into account infrared energy, temperature rise, chemical change, porosity, and dissipative effects. Also noticed is the relationship between the temperature profile and changes in the Eckert number, radiation parameter, magnetic parameter, and volume percentage of  $\text{TiO}_2$  and Ag nanoparticles. With increasing values of the chemical reaction parameter, the mass transfer and the unstable concentration number grow.



*Wahid et al.* [26] the primary focus of his work is on the mhd stagnation point flow (MHD) radiation flow of a hybrid aluminum oxide nanofluid via a porous plate with mixed convection. In contrast to the conventional nanofluid model, which takes into account an only type of nanoparticle, in our study, we take into account the hybridized of both types of nanoparticles, namely copper and alumina. When the copper concentration volume is reduced and the magnet and radiative parameters are multiplied, the existence of opposing flow caused by the combination of convection and radiation parameters can improve heat transmission. *Algehyne et al.* [27] his study examines how the hybrid nano liquid's thermal properties have increased. His research has taken into account the partially ionized hybrid nanofluid flow in three dimensions of the magneto hydrodynamic flow across a stretching sheet. Water and fuel oils are utilized as the basis liquids in which silver and graphite oxide nanoparticles are combined to create hybrid nanofluids. The flow model makes use of the Solvable in nonpolar mass and heat flux model. For lower thermal Biot numbers, the thermal properties of the nanofluids are weaker than for greater temperature Biot numbers. In contrast to the hybrid nanofluid based on kerosene oil, it is discovered that the liquid hybrid nanofluid is significantly affected by the embedded parameters. *Mourad et al.* [28] throughout his research, a water-based nanofluid ( $\text{Fe}_3\text{O}_4$ -MWCNT) was investigated numerically for its MHD natural circulation and entropy production properties in a permeable annulus between a heated Koch snowflake and a heated circular cylinder that had been treated to a consistent magnetic field. The unique shape and several analysed placements of the heat barrier highlight his work's originality. *Salmi et al.* [29] examines the interactions between the non-uniform magnetic field, Reynold porous medium, and Hall and ion slip currents under the dispersion of hybrid nanoparticles. Using conservation principles and correlations between the thermophysical characteristics of hybrid nanofluid and hybrid nanoparticles, the flow condition is turned into mathematical issues. It is seen through numerical simulations that fluid particle motion varies with Weissenberg number, and it is found that fluid motion slows down with better amounts of Weissenberg number. An increase inside the Darcy poroelastic parameter results in a significant slowing down of the fluid's motion since an increase suggests a decrease inside the porous medium's permeability. The fluid's ability to relax thermally allows it to maintain equilibrium temperature by avoiding temperature changes. As a result, a striking drop in the temperatures of the fluid showing signs of thermal relaxation is seen. Numerical investigations have also shown that Hall and ionic slip currents are what slow decrease the Ohmic dissipation process.

*Waqas et al.* [30] his study intends to examine the relevance of thermal radiation in the

presence of a nanofluid flow along a stanching surface and the function of heat source-sink. Here, copper, aluminium oxide, and graphite oxide nanoparticles are added to an ethylene glycolbase fluid. The results of his analysis demonstrate that the fluid velocity rises with higher variations in the Deborah number while falling with rising estimates of the magnetic parameters. The thermal distribution profile indicated increased performance for rising Biot number and thermal radiation while indicating falling performance for rising Deborah number variations. *Korei et al.* [31] investigated that to use fluid mechanics that uses numerical dynamics (CFD) methods, the lid-driven cavity problem involving magneto-convection flow is studied. This is accomplished by the cavity taken into account in this numerical analysis having two rounded corners, being slightly heated from of the bottom side, and being filled with an Upload and download hybrid nanofluid (HBNF). Several parameters are analyzed using streamline, isotherms, total entropy production, locally and average Nusselt numbers, and other techniques. The results of the data analysis showed that the temperature distribution and flow of the hybrid nanofluid are significantly influenced by the magnetic field orientation. The mean Nusselt (Num) and total entropy production were highest for the concentration ( $\text{Al}_2\text{O}_3$  75%, Cu 25%). (Sg). Moreover, as Ha and Ri increase, the rate of heat transfer and irreversibility decrease.

*Waini et al.* [32] his research focuses on a region of non-axisymmetric stagnation and point flow on a flat plate in a material that is porous with hybrid nanofluid flow by applying similarity-based variables. A few illustrations of the rate of heat transmission and friction proportion are also presented, in addition to the velocity and profiles of temperature. It's noteworthy to notice that the friction coefficient displays a pattern of symmetries in both the dimensions (x and y). Furthermore, the outcomes demonstrate that the friction coefficient rises when the parameters of the porous medium and hybrid nanoparticles rise. The heat exchange rate was increased by hybrid nanoparticles, whereas the fluid parameter had the opposite impact. Moreover, the shear-to-strain ratio value at which there is no friction on the surface is calculated. *Gangadhar et al.* [33] explores if hybrid nanofluid should be considered a different kind of nanofluid because of its thermal properties and potential use in heat transfer studies. The major objective of this study is to establish a connection between traditional and hybrid nanofluid qualities based on viscous incompressible, micro polar theory, and the outcome of heat heating over an exponentially stretched surface. Calculating velocity, micro rotation, and temperature field's graphs enables comparisons between the properties of blood of noble origin, MgO/blood the nanofluid and Au-MgO/blood nanofluid hybrid. Results of the

friction factor and Nusselt number are also presented for a more comprehensive understanding of flow and heat rate of transfer in nanofluids and hybrid nanofluids. Among the analysis's final conclusions is that the hybrid nanofluid's rate of heat exchange is 13.8 times higher as compared to the rest of the nanofluid. When micropolar impacts viscous dissipation, plus convection circumstances are present. Finally, compared to other nanoparticles, platelet-sized particles transport heat more quickly.

*Dawar et al.* [34] investigated that need for sun energy in the modern day, as well as the characteristics of ultraviolet lightness towards to the heat exchange of three-dimensional generalized magneto hydrodynamic with sodium alginate-based oxide  $\text{Fe}_3\text{O}_4$ -SA nanofluid flows via a spinning disc. Moreover, the Brownian motion, thermophoresis, and Arrhenius activation energy phenomena are considered. Compared to generalized nanofluid, sodium alginate-based iron oxide nanoparticles exhibits more fluctuation due to film width. The velocity profiles have decreased due to the larger magnetic parameter. Moreover, compared to  $\text{Fe}_3\text{O}_4$ -SA nanofluid, the generalized nanofluid has increased in velocity extraordinarily. The larger thermophoresis parameter, on the other hand, has increased the temperature while having the opposite effect on the concentration profile. Also, compared to  $\text{Fe}_3\text{O}_4$ -SA nanofluid, the generalized nanofluid has a higher variance in temperature profile; nevertheless, there is no difference in the concentration profile. The temperature profile has been enhanced by the increased absorption parameter, irradiance parameter, and thermal Biot number. Moreover, compared to  $\text{Fe}_3\text{O}_4$ -SA nanofluid, the generalized nanofluid's temperature profile rises noticeably.

*Vajravelu et al.* [35] search to investigate the flow and heat transmission properties of a viscous liquid above a nonlinearly stretching sheet, an analysis is conducted. The flow and heat transfer equations, which govern mass, momentum, and energy, are partially separated to use a similarity transformation that is distinct from the one used for the linearly stretched sheet problem. (In a specific case, though, the outcomes for the problem of a sheet that is linearly stretched can be found.) The flow is constantly from the stretch surface to the fluid, he discovered in addition. *Tsou et al.* [36] he describe the flows and temperatures fields inside the boundary layer on a continuously moving surface analytically and experimentally. Both turbulent and laminar flowing scenarios are covered in the inquiry. The boundary-layer temperature and velocity distributions' results as well as the interfacial and heat-transfer coefficients, are provided by the analytical solutions. The laminar velocity measurements

exhibit great agreement with the theoretical predictions, demonstrating that a flow that can be mathematically described as a boundary layer on a prolonged surface actually exists. Those of analysis and experimentally determined turbulence velocity profiles agree extremely well. Similar agreement is discovered for friction coefficients calculated using Clauser-plot techniques from the data. *Fang et al.* [37] he investigates a viscous flow across a rotating and stretching cylinder. The Navier—Stokes equations have an exact solution, and there is only one solution for each value of the flow Reynolds number that is given. According to the findings, the flow penetrates the surrounding fluid shallower at higher Reynolds numbers and velocity decays more quickly. To the atmospheric zero velocity, all velocity profiles algebraically decay. *Sprague et al.* [38] a extremely flexible cylindrical sheet performing pure torsional motion has its surrounding flow examined. The issue is controlled by the torsional Reynolds number  $R = a^2/\nu$ , where  $R$  is the cylinder's radius,  $\nu$  is the fluid's kinematic viscosity, and  $a$  is the axial rate of rotation. The primary flow's axial pressure gradient causes a mild transverse flow with in meridional plane, which is an intriguing aspect of the problem. Its motion's axial component manifests as a wall jet. The shearing stress parameters as well as the radially up flow asymptotics at high Reynolds numbers are provided and contrasted with comprehensive numerical results obtained for the broad range of Reynolds numbers value.  $10 - 2 \leq R \leq 10$ . *Seddeek et al.* [39] investigated heat transmission over a stretching surface with changing heat flux has been examined in relation to radiation and thermal diffusivity. The heat flux is believed to change as a linear relationship with temperature. Both the mathematical formulation for such temperature field and the accurate analytical solution for such velocity are provided. Several values of changeable heat transfer, radiation, temperature parameter, and Prandtl number are given numerical solutions.

*Hassan et al.* [40] the flow separation flow and heat exchange of an electrical conductor viscous fluid on a sheet that is stretching are the subjects of his study. By cutting the number of variables that are independent in the given system of differential equations with partials by one, a system of quasi ordinary differential equations results, which is used to determine the symmetric reduction for the governing equations. Plots of the data show the effects of different physical parameter values on the vertical and horizontal velocities, temperature, wall heat transfer, as well as the wall shear stress (surface friction). Furthermore, we observed that there is good agreement between the current results and those from reported numerical and homotopy approaches. *Qi et al.* [41] highlight the most recent advances in the miniemulsion generation of hybrid nanoparticles since 2009. Organic-inorganic, polymeric, and natural

macromolecule/artificial polymer hybrid nanoparticles are some examples of these hybrid nanoparticles. They can be created by miniemulsion (co)polymerization, simultaneously polymerization of monomers made from vinyl and vinyl-containing inorganic precursors, solvent displacement techniques, through the precipitation of preformed polymer compounds in the presence of inorganic constituents, or by grafting polymerization onto, from, or through natural macromolecules. Hybrid nanoparticles' characteristics, traits, and uses are also covered. *Aaron et al.* [42] describe a new technique for optical imaging that combines the benefits of plasmonic nanoparticles with molecular targeting and magnetic actuation. Hybrid nanoparticles that come with a gold coating covering an iron oxide core are used to create this combination. The growth factor epidermal receptor, a popular cancer biomarker, is the focus of the nanoparticles' infrared signal, while the gold component resonantly scatters visible light to produce a powerful optical signal. The contrast in photographic images of cells labelled using hybrid gold/iron nanoparticles of oxide is dramatically increased as a result of strong plasmon resonance (PR) scattering and magnetic actuation. *Devarajan et al.* [43] his work describe the CNT/Al<sub>2</sub>O<sub>3</sub> hybrid nanofluids' thermophysical characteristics for use in heat transfer applications. CNT and Al<sub>2</sub>O<sub>3</sub> nanoparticles were added in an equal amount to the starting fluid for two distinct levels of 0.05 & 0.1%. The thermophysical properties are improved by the addition of Al<sub>2</sub>O<sub>3</sub> nanoparticles to CNT nanofluid, according to the results. Although the heat conductivity of CNT itself improved by only 8% at the base fluid, hybrid nanofluids increased by 20% at an ultimate concentration of 0.1%. Similar to this, as compared to base fluid, hybrid nanofluid's density and viscosity increased by up to 10% and 7%, respectively. With an ultimate concentration of 0.2%, the particular thermal energy capacity of the hybrid nanofluids rises to roughly 138% that of CNT nanofluid.

*Esfe et al.* [44] investigations have been made on the fluid viscosity of four nanolubricants containing various ratios of carbon nanotubes (CNTs) and titanium (TiO<sub>2</sub>) nanoparticles (10%-90% and 55%-45%) in 10w40 engine oil. These nanofluids were created with a solid volume fraction of between 0.25 and 1 %, and they have been put to the test between 15 and 55 °C. The fluid shear rate was another variable that was looked at in order to understand the rheological behaviour of nanofluids. The impacts of temperature and particle volume fraction on the nanofluid are increase and decrease of viscosity, respectively. The viscosity of all sorts of nanofluids decreases by 80% or more as the temperature rises, and the type of nanoparticle being utilised has little bearing on this figure. Additionally, the viscosity of the nanofluids including MWCNTs at a solid volume proportion of 0.75% increases by

100%. According to the experimental findings, increasing the amount of carbon nanotubes in a nanofluid has a significant impact on the fluid's non-Newtonian behaviour, which in turn improves the shear-thinning behaviour of suspensions. *Yaseen et al.* [45] researchers have focused on the flow of a nanofluid between parallel plates. The focus has switched to hybrid nanofluid flows due to the rising energy needs and their applications, but there is still a great deal of research to be done. This analysis is carried out to investigate the symmetry of the hybrid nanofluid ( $\text{MoS}_2\text{-SiO}_2/\text{H}_2\text{O-C}_2\text{H}_6\text{O}_2$ ) and the MHD compressing nanofluid ( $\text{MoS}_2/\text{H}_2\text{O}$ ) flow across parallel plates. The field of magnetism, thermal radiation, thermal source/sink, suction/injection action, and porous medium are used to analyse the heat transport phenomenon. In the current model, the upper plate is moving towards the bottom plate, which is elongating with a straight velocity. Investigated is how the variables affect the fields of temperature and velocity, heat transfer rate, patterns of velocity boundary layers, and streamlines. The solution characteristics are discussed and displayed visually. Furthermore, compared to the ( $\text{MoS}_2/\text{H}_2\text{O}$ ) nanofluid flow, the number for Nusselt particles at the bottom plate is higher for the hybrid ( $\text{MoS}_2\text{-SiO}_2/\text{H}_2\text{O-C}_2\text{H}_6\text{O}_2$ ) nanofluid. The streamlines seem denser when suction or injection is present. The velocity boundary layer's region also has a thinning effect as a result of the magnetic field. The findings of this work have implications for a number of thermal systems, the field of engineering, and manufacturing procedures that use hybrid nanofluids and nanofluids for cooling and heating.

*Bayones et al.* [46] investigate to generate high temperatures, curved collectors for solar energy (PTSCs) are frequently employed in solar thermal systems. The goal of the current study is to understand how entropy develops and how nanosolid particles affect the shape of a parabolic trench surface collectors (PTSC) fitted on a powered by solar energy ship (SPS). In the current investigation, a porous medium, Darcy-Forchheimer effects, and the non-Newtonian first-degree viscoelastic type were all used. A non-linear stretch sheet caused the PTSC to flow, and the temperature flux in the thermal border layer was calculated using the variations in thermal conductivity, the heat source, and the effects of viscous dissipation. ( $\text{MoS}_2\text{-Cu/SA}$ ) nanofluids that are hybrids and copper-sodium alginate ( $\text{Cu-SA}$ ) hybrid nanofluids were employed as working fluids. The results demonstrated that the skin's friction factor increased while the Nusselt number decreased due to the permeability factor. Furthermore, the Brinkman number was utilised for tracking changes in viscosity, and the Reynolds number was used to increase overall entropy variance across the domain. Using  $\text{Cu-SA}$  nanofluid increased thermal efficiency by 1.3-18.8% as compared to  $\text{MoS}_2\text{-Cu/SA}$ .

*Nalivela et al.* [47] explain that on MHD spontaneous convective transfer of mass of an impermeable, viscous fluid flow via a stretching surface, the effects of viscosity dissipation and radiation are explored. The impact of non-dimensional factors on temperature, concentration, and velocity is investigated and graphically demonstrated. It has been found that as the impact of the chemical parameter, Schmidt number, Eckert number, radiation, as well as the magnetic parameter ( $M$ ) increase, the temperature profiles increase, however as these parameters increase, the velocity profile decreases. Additionally explored and organised in tabular form for various values of the chemical reaction, the magnetic field, as well as Schmidt number are the friction factor, Nusselt, as well as Sherwood numbers. The results of this investigation are widely accepted by modern scholarship. *Punith Gowda et al.* [48] thermal exchange mechanisms, nuclear reactors, electric coolers, and solar collectors all benefit from improved heat transfer. Selecting an appropriate nanofluid or ferromagnetic liquid as an active liquid will increase the rate of mass and heat transfer. In this regard, we have looked at the flow of a ferromagnetic nanofluid past an elastic flat sheet with a porous medium and a chemical reaction. Furthermore, the Koo as well as Kleinstreuer-Li (KKL) nanofluid concept is used to simulate and take into account nanofluid. Skin friction, Sherwood as well as Nusselt numbers, along with the graphic representations of the velocity, concentration, and thermal profiles, are found to provide an unambiguous grasp of the current boundary flow issue. As the ferromagnetic interaction parameter rises, the velocity gradient declines, but the thermal gradient rises as a result of heat generated by friction between fluid layers. The rate of transfer of heat and the slope in velocity are both slowed down by higher values of the porosity parameter.

*Eid et al.* [49] his one of the most important tasks for improving the transmission of heat is the use of hybrid nanoparticles instead of just nanoparticles. The analysis of the transfer of heat and flow caused by an exponentially decreased sheets of hybrid nanoparticles is the primary objective of this study. To create the  $\text{Fe}_3\text{O}_4\text{-Cu/EG}$  hybrid nanofluid, the copper (Cu) and magnetite ( $\text{Fe}_3\text{O}_4$ ) nanoparticles are suspended in ethylene glycol (EG). The impact of various variable parameters on velocity, temperature profiles, friction against the skin coefficient, as well as local Nusselt number is one of this study's most significant results. These parameters include permeability of porous media, stretching/shrinking parameter, heat production and absorption effect, slip, and a nanoparticle volume fraction. Additionally, consideration is given to the effects of radiation, MHD, the suction/injection parameter, and the Prandtl number. Through graphs and numbers, the impact of key physical characteristics is

investigated. In a case where the hybrid nanofluid can shrink or stretch, it is discovered that an increase in the concentration of nanoparticles made of  $\text{Fe}_3\text{O}_4$  accelerates the rate of heat transmission. *Aly et al.* [50] his study makes a contribution through investigating mixed convection in a cavity filled with inclined nanofluid and saturated with a partly layered non-Darcy porous material. Furthermore, suggested an enhanced version of the incompressible smoothed hydrodynamics of particles (ISPH) method because of the benefit of particle-based methods. Using the renormalization kernel function, the boundary conditions handling of the existing ISPH conduct was improved. In the current experiment, we made the assumption that a Cu-water nanofluid had formed inside the inclined hollow. A non-Darcy fluid with pores has been saturated in the upper part of the cavity. Here, the nanofluid and a porous medium layer are coupled using a single domain approach. The cavity's bottom wall is heated, while its top wall, which is chilled, is moving at a tangential unit velocity. At zero velocity, the other two walls sides are adiabatic. Here, we examined at how a Cu-water nanofluid's capability to transmit heat was affected by the Richardson parameter  $\text{Ri}(0.0001-100)$ , the Darcy parameter  $\text{Da}(105-102)$ , an inclination angle  $\alpha(0-90)$ degree, and various solid volume fractions  $\Phi(0-0.05)$ . The collected data indicated that when the Richardson number rises, the average number calculated by Nusselt drops. The general heat transfer rate was somewhat enhanced by the addition of 1-5% Cu nanoparticles.

*Aly et al.* [51] in a hybrid nanofluid with partial slide and viscous dissipation, the constant stagnation point flows and transfer of heat over a stretching/shrinking surface were theoretically and computationally investigated. It emerged that the hybrid nanofluid performs more effectively as a cooler on growing Eckert number, stretching, and slip parameters but operates better as a heater when the magnetic parameter is increased. Critical zones of a single or dual solutions have been proposed for shrinking sheets. Three zones of stability were identified while analyzing the constancy of the unique/dual solution. It was concluded that in the dual solution area, the velocity and elevation are significantly available closer to the terminated line. Additionally, it was demonstrated that they behave entirely differently in each of the three stable zones. *Salawu et al.* [52] investigated that nonlinear radiation and convection and radiation of the Maxwell nanoliquid flows in porous medium with the Arrhenius kinetic reaction in MHD heat and mass transfer. The Maxwell model is used to explain non-Newtonian fluids, and an Arrhenius pre-exponential kinetics are used to guide the creation of species molecular mixtures. An infinitely slippery plate with a significant amount of tension that may prevent material distortion is where the reaction mixture happens. The findings demonstrate



that the material term minimises the flow momentum whereas nonlinear heat radiation and convection increase it. Temperature ratio as well as viscous heat have an important effect on the pace of heat transfer, while Lewis numbers, molecular Brownian motion, and chemical reaction term promote species mass transfer. As a consequence, research on activation energy is essential for the dispersion of binary chemical mixes that move species and energy, helping chemical engineers and others in their efforts to prevent reactions blowup. *Adigun et al.* [53] examined the flow of a viscoelastic nanofluid through an inclined cylinder stretching linearly is covered in this communication's discussion of the magneto hydrodynamic (MHD) Stagnation region flow. Considered is a modified version of Darcy's law that takes Arrhenius activation energy into account. The fluid is conducting electricity and in a uniform magnetic field, and the cylinder wall is stratified in terms of both temperature and concentration. By using similarity transformations and the Spectral Local Linearization Procedure (SLLM), the PDEs boundary value problem is reduced to an ODE problem, and the resulting equations' solutions are achieved. Graphs are used to discuss the effects of suitable parameters on the fluid's velocity, temperature, and concentration. Tables are also used to explain their impacts on the skin-friction factor, Nusselt, and Sherwood values. The modified Darcy parameter is starting to show up., which has lowered nanofluid velocity and decreased the overall thickness within the boundary layer. The species concentration inside the flow system was observed to be reduced by both heat and solutal stratification factors. The activation energy additionally increased the nanofluid's species concentration levels.

*Hamzah et al.* [54] their work using the Galerkin Finite Elements Method, or GFEM, convection in combination with entropy generation is modelled in a porous enclosure driven by a wavy lid and loaded with a CNT-water the nanofluid in a magnetic field. A pair of unique instances of boundary situations for hot and also cool walls are utilised under account in order to examine the flow of fluid (streamlines), the movement of heat (local and average Nusselt numbers), and the generation of entropy parameters. In his research, the parameters such as Richardson (Ri), Darcy (Da), Hartman angle , The amplitude (A), The number of rises (N), volume fraction, the production of heat factor, Hartmann number (Ha), and the Reynolds number ( Re ) were explored. The outcomes demonstrated that raising the inclination of a magnetic field reduces the Nu values for low Richards numbers but increases them at higher Richardson numbers. *Labib et al.* [55] in his paper, a new idea of heat transfer improvement is presented through the investigation of forced convective transfer of heat of nanofluid using a two-phase mixture model. To examine how base fluids affect convective heat transfer

blending of  $\text{Al}_2\text{O}_3$  nanoparticles, two distinct base fluids are used separately. In the example of  $\text{Al}_2\text{O}_3$ /water nanofluids, the computational approach has been effectively validated using the experimental data that has been released in the literature. The findings indicate that Ethylene Glycol as the base fluid enhances heat transfer more effectively than water.  $\text{Al}_2\text{O}_3$  nanoparticles are mixed with CNTs and water the term "nanofluids" refers to a novel idea of combination or hybrid nanofluids the fact that can effectively improve convective heat transmission. Comparing the outcomes with experimental data published in literature allowed researchers to validate the mathematical framework for the CNTs/water nanofluid. The new notion of mixed nanofluids was then simulated with the tested method. Combining CNTs and  $\text{Al}_2\text{O}_3$  nanoparticles in a water base fluid has the tendency to considerably improve convective heat transfer performance. Due to the enhanced shear thinning characteristic of CNTs nanofluid, which makes the boundary layer thinner, considerable convective heat transfer expansion occurs in these areas.

*Lund et al.* [56] Investigated is the unstable magneto hydrodynamic (MHD) flow of a  $\text{CuAl}_2\text{O}_3$ /water hybrid nanofluid (HNF) in the presence of a radiant heat effect on a stretching/shrinking sheet. Both quantitatively and graphically, the results are compared to the published literature, and there is good agreement. Particularly shown graphically and conceptually are the implications of numerous new physical regulating variables on the profiles of speed, temperature, friction on the skin coefficient, and heat exchange rate. The numerical findings indicate that dual solutions are present for a certain set of magnetic, the suction, and instability parameters. Additionally, it was discovered that as the solid volume proportion of Cu is raised, the numbers of  $f''(0)$  grow in the initial solution and decrease in the second. After doing an analysis of the solutions' temporal stability, it is determined that only the first response is stable. *Sreedevi et al.* [57] in this field of her research, she investigates the unsteady magneto hydrodynamic transfer of heat and mass of a hybrid nanofluid flowing across a stretching surface with suction, chemical reactions, slip consequences, and thermal energy. Water is recognized as the basis fluid for hybrid nanoparticles, which are composed of carbon nanotubes and silver. The results of calculations are displayed on graphs to show how various relevant variables influence the temperatures, concentration, and profile of velocity of fluids. Tables listing the results and non-dimensional heat, mass, and velocity transfer values are also included. The temperature sketches of the nanofluid hybrid rose in both stable and unstable situations as the volume percentage of both nanoparticles increased. *Nabwey et al.* [58] the brief magneto hydrodynamics travel by way of the boundary layer of a not an Newtonian

micropolar the nanofluid using hybrid properties ( $\text{Fe}_3\text{O}_4$  -Ag) consumed with conducting micrometre evenly sized particles nanoparticles in a sheet of stretching close to stated surface temperature (PST) and enforced heat flux (PHF) cases is the subject of a thorough study by him. The results for a number of characteristics that affect how micropolar the nanofluid hybrids and particles behave during the phase transition are assessed, shown in graphical form, and then thoroughly described in tables. The accuracy of the computations has been demonstrated by comparing the acquired results to previously made available data. A rise in thermal relaxation strengthens temperature fluctuation in the micropolar the nanofluid hybrid and particle stages.

*Ajibade et al.* [59] examined that the impacts of boundary thickness of the plate and the dissipation of viscous on the constant airflow flow of an indestructible viscous liquid with variable characteristics are theoretically examined in this paper. This is because various investigations in the literature have failed to account for the thickness as well as the makeup of the boundary plates, and as a result, their conclusions are either exaggerated or understated. It was presumed that the thermal conductivity and viscosity of the energy absorbing fluid were temperature-dependent. Graphs and tables were used to demonstrate how the thermophysical and fluid parameters affected the results. The study has shown that as thermal conductivity rises, the velocity profile does as well. It was found that increasing boundary plate thickness causes the temperature near the heated plate to drop as the flow of fluid across the medium increases. Additional findings show that the rate of heat transfer drops on both plates with a rise in boundary thickness while the skin friction reduces on both plates with an increase in the viscosity of the fluid and boundary plate thickness. While a drop was seen with a rise in boundary plate thickness, it was determined that the volume flow rate increased with an increase in Brinkman number. *Huminic et al.* [60] in his work he investigate, novel hybrid nanoparticle aggregates with separate silicon and iron nanophases were employed to boost the base fluid's thermal conductivity. The pyrolysis laser process was used to create the hybrid aggregates, and they were evaluated using XRD, TEM, and HR-TEM evaluations. The hybrid nanofluid's thermal conductivity was assessed at various temperatures between 20 and 50 °C and mass concentrations between 0.25 and 1.0%. Based on the experimental findings, a new correlation was constructed to describe Fesingle bondSi hybrid nanofluids' thermal conductivity variations with temperature and mass concentration. The outcomes of the experiment were compared with experimental data from the literature. Additionally, the correlations put up by various scholars to predict the thermal conductivity of the hybrid

nanofluids have been contrasted and analysed. In accordance with the findings, thermal conductivity rises with temperature and concentration.

*Hussain et al.* [61] in this work homogeneous and heterogeneous responses in nanofluid hybrid flow were investigated under the effects of temperature-dependent viscosity variations, mixed convection, and magneto hydrodynamics. Stretchable cylinders are causing the flow of the fluid. Through the use of a heat source, thermal radiation, and viscous dissipation, the mechanism of heat transfer has been explored. Additionally, thermal feature inspection has been performed with the melting boundary condition. To control solute concentration, a straightforward isothermal model was used in the study. The base of the fluid is thought to be mostly made up of a homogeneous combination of MoS<sub>2</sub> nanoparticles. Velocity, temperature, concentration, skin friction, and Nusselt number have been compared between nanofluid and hybrid nanofluid in contrast to shape factors and embedding variables. The bvp4c matlab solver handles the resulting boundary layer issues for stretching cylinders. The study's conclusions demonstrated that a greater melting variable increases the thickness of the thermal boundary layer. When comparing hybrid nanofluid to nanofluid, it is seen that the flow and concentrations distributions are more stated, while the temperature trend is in the opposite direction. Additionally, for both types of fluids, a higher percentage of volume increases skin friction and the Nusselt number. When a bigger curvature variable is taken into account, drag coefficient and the transfer of heat at the cylinder's surface rise for nanofluids as opposed to hybrid nanofluids. This study shows that greater melting and temperature-dependent viscosity parameters boost heat transfer. When compared to other nanoparticles, the presence of blade nanoparticles (8.6) in the base liquid maximises the drag coefficient as well as heat transmission for both fluids. *Jana et al.* [62] worked on numerous nanomaterials' naturally high thermal conductivity has the potential to significantly improve fluidic transfer of heat applications. The thermal conductivity of fluids was enhanced in this study using conductive nanomaterials including copper nanoparticles (CuNPs) carbon nanotubes (CNTs) and nanoparticles of gold (AuNPs), as well as their hybrids like CNT-CuNP or CNT-AuNP. The greatest increase in thermal conductivity was seen in mono-type nanoparticle solutions, and the enhancement using CuNPs was the highest. But hybrid suspensions weren't showing the same level of development. Several nanofluids' measured thermal conductivities regularly exceeded the theoretical forecasts made by preexisting models. Discussion is had regarding the mechanisms increasing thermal conductivity. By using a UV-vis-NIR spectrophotometer to measure nanofluid stability, it was found that the degree of stability was affected by the properties of

the nanoparticles.

*B. Johnson et al.* [63] a porous medium with an interaction of heat power, heat generation/absorption, and move thermo effect as well as the presence of thermal diffusion and chemical reaction was used to study how various patients act in a non-Newtonian kind of Walters' B fluid model. To execute the translated equations, one uses the Homotopy Analyse Procedure (HAM). Thus, the significance of the magnetic variable, the nearby Weissenberg numbers, and other observed parameters are examined. One significant finding is the variation in the heat buoyancy variable, which speeds up the fluid's motion and significantly reduces the issue's temperature, cooling the system and more electronic components in the science-related field, whereas the quiescent fluid obtained thermal impact due to the presence of powerful convective radiation in different levels of the convective heat transfer parameter, which aids in drying out materials in the technological-related fields.

*Roy et al.* [64] the effect on a binary chemical reaction dictated by activation energy on the transmission of heat and mass of a nanofluid that is a hybrid flow via a permeability stretched surface was investigated within a predetermined timeframe, two solutions emerged whenever the suction variable was fixed. The results show that as the amount of dual solutions increases, the volume percent of copper nanoparticles, the Richardson's number, and the sum of the buoyancy forces parameters all increase. The contrary is seen when the parameters for stretching, temperature difference, and aluminum nanoparticle volume fraction increase. Local Nusselt number, skin friction coefficient, Sherwood number, Richardson's number, volume amount of copper nanoparticles, and combined buoyant forces parameter rise together with the suction parameter, Richardson's numbers, and combine buoyancy forces parameter a tiny amount of the dimensionless activation energy is required for the mass transfer, which gets more pronounced as the fit rate stable, differential variable, temperature and non-dimensional reaction rate increase. The flow properties are significantly influenced by changes in the stretching parameter, suction parameter, and nanoparticle volume fraction. *Sulochana et al.* [65] in addition to a constantly shifting needle submerged horizontal in the flow field, his work presents the outer layer examination of a magneto hydrodynamic nanofluid hybrid (Al-Cu/methanol) flow. It presumes that thermal radiation is either linear or nonlinear. The Sakiadis (quiescent fluid) condition is used to inspect the behaviour of the boundary layer. The wall friction and thermal transfer computations are tabulated and analysed in accordance with their results. Graphical representations of the designation of velocity and heat fields are investigated.

It was possible to achieve simultaneous solutions that demonstrated the superiority of the hybrid aluminum-copper/methanol nanofluid over the methanol-based Al-Cu alloys nanofluid (which contains 50% aluminium + 50% copper). An increase in needle diameter has a greater impact on the hybrid nanoliquid's rate of heat transmission. Further, nonlinear radiation from heat has a much greater impact on thermal profile than straight thermal radiation.

*Hosseinzadeh et al.* [66] this study used a two-dimensional Darcy-Forchheimer framework with a convectively heated plate to examine the chemically reactive radiated flow. Joule heating and heat production are used to analyse nonlinear thermal radiation. Additionally, porous medium flows are related to the Darcy-Forchheimer equation. Figures were also used to illustrate an additional concrete understanding of the characteristics. The Prandtl number was discovered to have a direct impact on the temperature and Nusselt number and whereas the Eckert number had the reverse effect. *Rahimi et al.* [67] described that Polymer-hybrid nanosystems have special qualities that make them useful in a variety of industries, including biological applications. Many recent research papers have focused on hybrid substances, which are made of polymers and inorganic or organic base systems. The results have demonstrated significant increases in drug targeting. By creating hybrid polymer materials, it is possible to avoid the costly and laborious method of creating new molecules, which can take years to perfect. The combination of properties in a hybrid system may result in a number of advantages over non-hybrid platforms, including longer circulating times, collapse of structure, high stability, rapid release, low encapsulation rates, and generic releasing kinetics. The purpose of this overview is to quickly and precisely describe the current state of knowledge about the application of polymer-hybrid nanomaterials in biological platforms. This review also focuses on the final addresses used in the synthesis processes and in the *in vitro/in vivo* applications.

*Kempannagari et al.* [68] the current project investigates the magneto hydrodynamic stagnation point movement of a micropolar fluid across an exponential curved surface and its convective transfer of heat characteristics. It is intended for the flow to be considered time-independent and laminar. Radiation effects, erratic heat sources and sinks, Joule heating, and fluctuating thermal conductivity are all thought to. To graphs are made to explore the impacts of different non dimensional parameters on various levels of speed, microrotation, as well as temperature.. With the Eckert number and varying heat source/sink features, we may identify a rise in temperature. Additionally, it's encouraging to note that the Nusselt number in the neighborhood increases at the same rate as Bio.

*Singh et al.* [69] examining the behavior of a magneto hydrodynamic elastic-viscous fluid's movement across a vertically oriented magnetized surface in a uniform permeability regime with magnetic and thermal diffusions is the main purpose of this study. In the case of a significant magnetic domain, the fluid becomes partially ionized and permeable, allowing it to flow. So, in this inquiry, the Hall current impact is taken into account. This study also examines the impact of rotating and imposed magnetic field on flowing nature. A remarkable finding reveals that magnetic diffusion enormously modifies the magnetic drag force to control the fluid flow. The fluid velocity rises as a result of mass diffusion. Additionally, observed that magnetic diffusion and the mass diffusion factor considerably diminish the outermost density of current along the main flow direction. *Abu Bakar et al.* [70] the primary goal of this study is to examine how a hybrid nanofluid moves through a porous, permeable Darcy medium that is subject to fall, radiation, as well as shrinking sheet Since the start of the millennium, hybrid nanofluid and its thermophysical properties have been studied. In this case, Cu/water operates as the fundamental nanofluid, and Al<sub>2</sub>O<sub>3</sub>-Cu/water functions as the two distinct fluids. The non-uniqueness of answers, which makes it difficult to find an answer that is bigger than any other between both the lower and upper branches, is found to occur over a range that encompasses the shrinking parameter. One can see from the analysis how the hybrid nanofluid has a higher rate of heat transfer than the regular nanofluid. The findings of the consistency for solutions show that the greater solution (first branch) is stable while the lower solution (second branch) is unstable.

## 2.1 Research Objectives

In this research our main objectives are:

- Investigation of the thermal conduction improvement due to hybrid nanoparticles.
- Flow field behavior with modifications to physical parameters, like magnetic number.
- Impact of the stretching of sheet on the flow and heat transport.
- Calculation of shear stresses due to increase in particles fraction in the fluid.
- Investigation of transport mechanism such as single nanoparticle-containing nanofluids, ethylene glycol, water, and oil.

## **2.2 Significance of the study:**

- In comparison to more traditional fluids used for heat transfer, such as single nanoparticle-containing nanofluids, ethylene glycol, water, and oil, hybrid nanoparticles perform better in terms of heat transfer.
- Hybrid nanoparticles are effective at cooling areas with a wide temperature range and a variety of thermal applications.
- Among the primary research areas for hybrid nanofluids are, refrigeration as well as heating, solar power, Heat exchangers uses for electronic cooling, heat pipes fluids in manufacturing and machining, ventilation, and air conditioning. The main goal of adopting hybrid nanofluids is to further improve the thermal characteristics of heat transmission of convectonal fluids.



## **CHAPTER 3**

### **PRELIMINARIES**

#### **3.1 Basic Definitions and formulas**

For a better comprehension of the analysis in later chapters, this chapter includes several common definitions, formula's and laws.

##### **3.1.1 Fluid**

Whenever an external force is exerted to the fluid which can be either something liquid or a gases, it keeps on moving and deform despite the modest resistance to the shearing force.

##### **3.1.2 Fluid mechanics**

The branch of physics known as fluid mechanics is focused on the forces acting on and within fluids (liquids, gases, and plasmas).there are two types of it.

##### **3.1.3 Fluid statics**

The branch of science called fluid mechanics that discusses the properties of fluids at rest.

##### **3.1.4 Fluid dynamics**

The area of fluid dynamics that analyzes how forces impact a fluid's properties.

### 3.1.5 Density

The ratio of mass to volume is how density is defined. It is can be expressed as;

$$\rho = \frac{m}{v},$$

(3.1)

SI unit of density is  $kg/m^3$ .

### 3.1.6 Pressure

Pressure is defined as the force to area ratio.

Mathematically it is defined as.

$$P = \frac{F}{A},$$

(3.2)

S.I unit of Pressure is  $N/m^2$ .

### 3.1.7 Stress

An external force *operating* across an object's cross section is measured by stress.

$$Stress = \frac{Force}{Area},$$

(3.3)

In the SI system, stress is expressed as  $kg/m.s^2$  and its dimension is  $\left[\frac{M}{LT^2}\right]$ . It has two different parts.

### 3.1.8 Shear stress

According to the definition of shear stress, this type of stress occurs when a force operates perpendicular to the material's cross section.

### 3.1.9 Normal stress

When a force is applied consistently across a material's cross section, a type of stress defined as normal stress emerges.

### 3.1.10 Strain

Strain refers to the relative deformation of a material when a force is applied to that though. It doesn't have any dimensions.

### 3.1.11 Viscosity

It is a phenomenon of fluids that keeps them resistant to deformation and has to do with the internal friction between the fluid layers. The methodologies to define viscosity are as follows:

### 3.1.12 Dynamic viscosity

The quantity of shear stress to velocity gradient is known as absolute viscosity or dynamic viscosity. Dynamic viscosity is represented by  $\mu$ , SI units is  $kg/m.s$  and its dimension is  $\left[\frac{M}{LT}\right]$ .

### 3.1.13 Kinematic viscosity

Kinematic viscosity refers to the relationship between dynamic viscosity and fluid density. It is denoted by  $\nu$ . In mathematically it can be expressed as;

$$\nu = \frac{\mu}{\rho}, \quad (3.4)$$

Measurement of kinematic viscosity is  $\left[\frac{L^2}{T}\right]$  and it has a unit  $m^2/s$ .

### 3.1.14 Newton's law of viscosity

It demonstrates that the shear stress of the fluid is directly and linearly related to the velocity gradient.

Mathematically expressed as;

$$\tau = \mu \frac{du}{dy}. \quad (3.5)$$

### **3.1.15 Newtonian fluids**

Newtonian fluids have advanced significantly in the study of turbulence and multi-phase flow in fluid dynamics. The majority of low molecular weight materials, including molten metals and salts, organic and inorganic fluids, solutions of minimal molecular weight inorganic minerals, etc., show shear stress that is proportional to their rate of shear at a constant pressure and temperature. This constant of proportionality is viscosity. These fluids are commonly referred to as Newtonian fluids. For example water, air etc.

### **3.1.16 Non-Newtonian fluids**

Non-Newtonian fluids are ones that do not follow Newton's viscosity law or for which the relationship among strain and shear stress rate is nonlinear. Viscoelastic non-Newtonian fluids come in a wide variety of forms that can be examined, including polymers, thermoplastics, granular substances, paints, gel-like substances, and biological fluids.

### **3.1.17 Flow**

Flow is the term used to describe the amount of fluid that travels across an area in a specific amount of time.

### **3.1.18 Incompressible flow**

A flow that is not compressible is a situation in which the fluid component's density remains constant over the course of the flow.

### **3.1.19 Compressible flow**

When a fluid's density changes as it is flowing, a form of flow known as compressible flow takes place.

### 3.1.20 Laminar flow

Laminar flow occurs when fluid particles move in parallel layers or along preset trajectories without colliding.

### 3.1.21 Turbulent flow

A flow in which the fluid particles move randomly and without following to any preset patterns is known to as a "turbulent flow."

### 3.1.22 Steady flow

When the fluid properties at a location (such as pressure, weight, velocity, etc.) do not depend on or are independent of time, the flow is said to be stable.

$$\frac{\partial \psi}{\partial t} = 0, \quad (3.6)$$

where  $\psi$  shows fluid's property.

### 3.1.23 Unsteady flow

Unsteady flow is a flow when the fluid characteristics (such pressure, density, and velocity) change overtime at a specific place.

$$\frac{\partial \psi}{\partial t} = 0, \quad (3.7)$$

### 3.1.24 Viscous Nanofluid

A nanofluid is a fluid that contains nanoparticles, also known as nanoparticles. Nanofluids are beneficial for heat transfer in a variety of applications, such as microelectronics, fuel cells, hybrid engines, and more. The nanoparticles employed in nanofluids are often comprised of metals, oxides, which are carbides, or carbon nanotubes.

### 3.1.25 Hybrid Nanofluid

Advanced types of nanofluids called hybrid nanofluids are created by mixing two or more nanoparticles with a base fluid. According to nanofluid, it increases heat conductivity significantly. Examples are;

Hybrid nanofluids have extensive applications in various areas of heat transfer such as automotive cooling system, heat pipes, refrigeration etc.

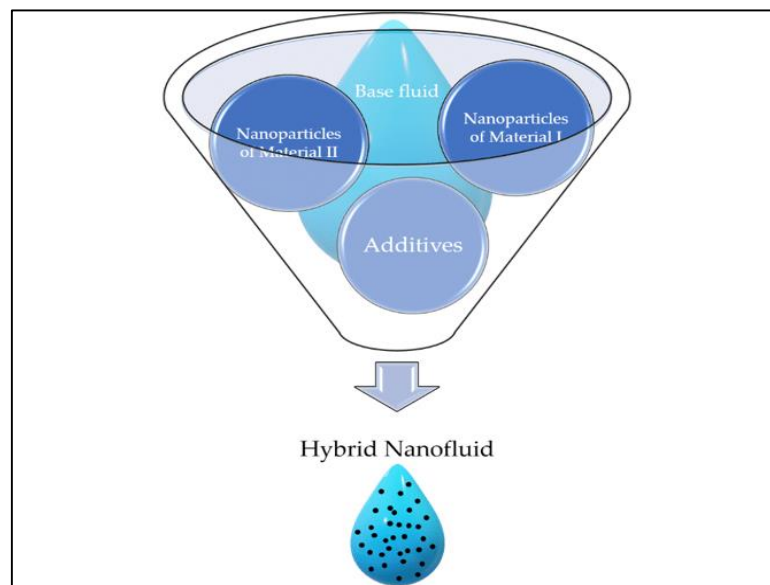


**Figure 3.1:** Hybrid Nanofluid

### 3.1.26 Stagnation Point

In flow field, Stagnation point is point where fluid have zero velocity.

### 3.1.27 Stagnation point flow

Stasis point flow is the term used in fluid dynamics to describe a fluid's movement right up against a solidsurface. When the fluid gets close to the surface, it separates into two streams.

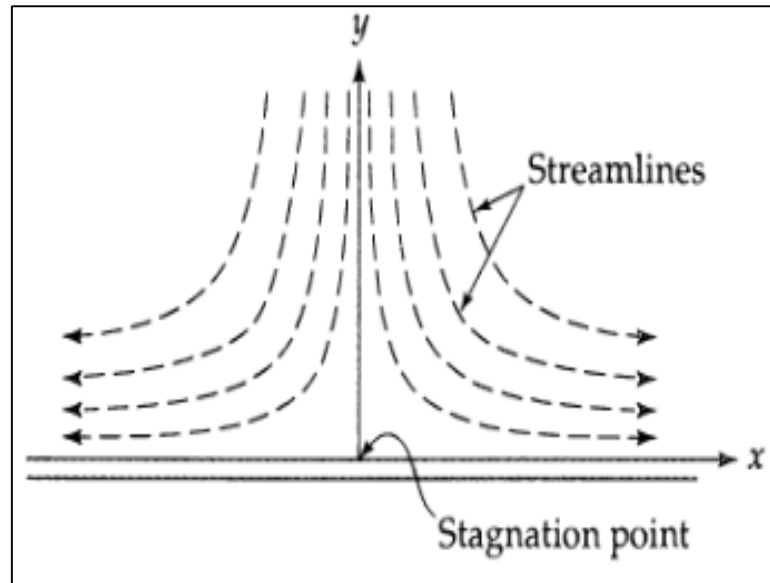


**Figure 3.2:** Stagnation Point

### 3.1.28 Thermal Conductivity

Thermal conductivity is the energy transfer resulting from molecules resting motion over a temperature gradient.

$$k = \frac{QL}{A\Delta T}, \quad (3.8)$$

Thermal conductivity is represented by  $k$ ,  $Q$  is heat flow,  $A$  is area and  $L$  is unit thickness of material and  $\Delta T$  is temperature difference. Its S.I unit is  $kg.m/s^3$ .

### 3.1.29 Thermal diffusivity

Thermal diffusivity is calculated by dividing it by the density of specific heat per unit. It can be written as;

$$a = \frac{k}{\rho C_p}, \quad (3.9)$$

As  $k$  show thermal conductivity,  $\rho$  denoted for density, heat Capacity is denoted by  $C_p$ .

### 3.1.30 Modes of heat transfer

There are three ways to transport heat. Such as;

- **Convection**

Heat is transferred by a fluid, for example water or gases, through convection.

- **Conduction**

Conduction is the direct flow of energy from a single molecule to another. For example a lizard on a rock warming its belly. Touching the ice and feeling your hand freeze.

- **Radiation**

Heat can be transmitted by electromagnetic waves, called radiation. For example X-rays from an X-ray tube, gamma rays, which come from radioactive substances, and microwave from an oven

### 3.1.31 Viscous Dissipation

When a viscous fluid flows, the fluid's motion creates kinetic energy, which the fluid's viscosity absorbs and converts to internal energy. Viscous dissipation is the term used to describe this phenomenon, which is regarded as irreversible.

### 3.1.32 Magnatohydrodynamic (MHD)

Magnetohydrodynamics is a method for analysing how electrically conducting fluids move when a magnetic field is present.

Magneto-hydro-dynamics (MHD) is a name that combines the terms "magneto," which denotes to a field of magnets, "hydro," which implies fluid, and "dynamics," which indicates motion.



### 3.1.33 Heat generation/absorption

The conductor produces heat when electric current flows through it. This process is known as Joule heating, also known as thermal resistance or Ohmic heating. Joule heating improves the method of heat transfer to lower dynamic viscosity, which causes an increase in electrical conductivity.

### 3.1.34 Lorentz force

The force applied to a charged particle as it is travelling through a magnetic field and an electric field. The Lorentz force is the term used to describe the entire electromagnetic force  $F$  operating on the charged particle. Mathematical representation is;

$$\vec{F} = q(\vec{E} + \vec{V} \times \vec{B}). \quad (3.10)$$

### 3.1.35 Fouier's law

Fourier's law says, the region at right angles to the gradient through which heat flows is directly proportional to the negative slope of temperature as well as the time it takes for heat transfer. Fourier's law is known as the law of heat conduction.

$$q = -k \nabla T. \quad (3.11)$$

### 3.1.36 Brownian motion

Tiny particles in a fluid moving randomly and erratically as a result of constant bombardment from molecules in the environment.

### 3.1.37 Buoyancy force

The tendency of a fluid to apply a lifting force on an item that is partially or completely submerged in that fluid is known as buoyancy force.

The buoyant force in S.I. is measured in Newtons.

## 3.2 Dimensionless numbers

### 3.2.1 Reynolds number

The Reynolds number is the ratio of inertia forces to viscous forces when a fluid experiences relative internal motion as a result of different fluid velocities.

In low Reynolds number flows, laminar (sheet-like) flow often predominates, whereas in high Reynolds number flows, turbulent flow typically predominates. A variety of scenarios, such as liquid flow through pipelines and air flow over aviation wings, call for the usage of the Reynolds number.

It is utilised to compare similar but different-sized flow scenarios, such as the size difference between a wind tunnel model of an aeroplane and the actual aircraft, and to predict the transition from laminar to turbulent motion. Mathematical expressions are;

$$Re = \frac{\rho u L}{\mu}, \quad (3.12)$$

where,  $\rho$  is density of fluid,  $u$  represent the flow rate,  $L$  shows characteristic linear dimensions, and  $\mu$  Dynamic defines viscosity as a fluid's characteristic.

### 3.2.2 Lewis number

It has no dimensions and is produced by the mass-to-heat diffusivity ratio.

Calculating the density of the concentration boundary layer involves comparing Lewis numbers with both the concentration boundary layer and the thermal boundary layer thickness. Mathematical expressed as;

$$Le = \frac{\text{thermal diffusion rate}}{\text{mass diffusion rate}},$$

or

$$Le = \frac{\alpha}{D}. \quad (3.13)$$

### 3.2.3 Prandtl number

The relationship between the diffusivity of heat and momentum is described by the non-dimensional Prandtl number ( $k$ ). In simple terms, the proportion of a fluid's dynamic viscosity to its thermal conductivity.

The Prandtl number is expressed mathematically as follows:

$$Pr = \frac{\text{viscous diffusion rate}}{\text{thermal diffusion rate}},$$

or

$$Pr = \frac{c_p \mu}{k}, \quad (3.14)$$

where  $C_p$  represent specific heat at constant pressure, thermal conductivity is  $k$  and dynamic viscosity is denoted by  $\mu$ .

### 3.2.4 Eckert number

A dimensionless quantity called the Eckert number ( $Ec$ ) is employed in continuum mechanics. It describes the connection among a flow's kinetic energy as well as the difference in boundary layer enthalpy. The Eckert value is used to describe how heating itself of a fluid as a result of dissipation effects influences it. Mathematical expression;

$$Ec = \frac{\text{Kinetic energy}}{\text{Enthalpy}},$$

or

$$Ec = \frac{v^2}{c_p \Delta T}, \quad (3.15)$$

The Prandtl number plus Eckert number are combined to determine the viscous nature of energy waste whenever flow speed is low.

### 3.2.5 Nusselt number

The ratio of fluid conduction transfer of heat to convection heat transfer under identical circumstances is known as the Nusselt number. The channel influence and the boundary condition for wall heat transfer determine the Nusselt number, which is constant in fully developed laminar flow.

$$NuL = \frac{\text{convective heat transfer}}{\text{conductive heat transfer}},$$

or

$$NuL = \frac{hL}{k}, \quad (3.16)$$

here  $h$  represent coefficient of heat transfer,  $L$  stands for the usual length and  $k$  for the thermal conductivity of the fluid. If the Nusselt number is one, laminar flow will be represented by a slow motion that is seen to be advantageous when contrasted to pure fluid conduction. If the Nusselt number is set to a high value, an efficient convection is observed, which is evident in turbulent pipe flow and results in  $Nu$  with orders between 100 and 1000.

### 3.2.6 Skin friction

The type of friction brought on by a fluid flowing in relation to a solid surface is referred to as skin friction.

Mathematically, the skin friction coefficient is expressed as

$$C_f = \frac{\tau_w}{\frac{1}{2}\rho U^2}, \quad (3.17)$$

As density is denoted by  $\rho$ ,  $U$  represent velocity and the shear stress at the wall is  $\omega$ .

### 3.2.7 Conservation laws

- **Mass equation**

For fluids with constant densities, mass is conserved inside a control volume. Furthermore to any mass gathering inside the control volume, the total amount of mass reaching the control volume must be equal to the total mass quitting the control volume.

It can be expressed as;

$$\nabla \cdot (\rho V) = 0. \quad (3.18)$$

- **Momentum equation**

To calculate the force as a stream of fluid that flows ultimately puts against the boundaries of the flow route as the fluid changes direction, velocity, or both momentum in a linear equation in fluid mechanics, Newton's second law is frequently referred to as the linear momentum equation.

Mathematically expressed as;

$$\rho \frac{dv}{dt} = (\nabla \cdot \tau). \quad (3.19)$$

- **Energy equation**

The net flow of energy into or out of a system throughout a process must be equivalent to the system's change in energy content. Mathematically it can be expressed as;

$$\frac{dT}{dt} = -\nabla \cdot q \quad (3.20)$$

## CHAPTER 4

### **Hiemenz stagnation-point flow with heat transport over bi-directional stretching sheet under magnetic field**

#### **4.1 Introduction**

Using a bi-directional stretching sheet, investigation are conducted with the effects of heat and mass transfer that occurs in normal impingement of a viscous nanofluid in the Hiemenz stagnation-point flow. Weidman (2018) examined the Hiemenz stagnation-point flow over the biaxial extending sheet in a recent work. For various amounts of  $\alpha$  (streamwise stretching rate) and  $\beta$  (cross-stream stretching rate) solutions have been found in this study. The current work investigates the process of heat and solutal energy transfer through the Hiemenz stagnation-point transfer of nanoliquid under thermophoretic and Brownian forces. The bvp4c numerical technique is used to calculate the results of related ordinary differential equations (ODEs) for energy transfer in viscous nanofluid flow. Physical reasoning is also provided via graphically outcomes with the influence of parameters without dimensions on the field of flow as well as energy transportation. The results show that the flow field declines as you increase the Lorentz force in the cross-stream and vertical directions, however contradicting nature is observed for the streamwise velocities factor. Energy is transported more efficiently in the viscous fluid Hiemenz flow due to thermophoresis and Brownian movement of nanoparticles. The variables of a previous study's shear stress examination are used to validate the findings of the presentone.

#### **4.2 Mathematical Formulation:**

A weak, viscous stream impinge a flat, stretchable surface normally. The sheet is positioned in the  $z = 0$  plane and the surface is stretching in two directions with linear velocities of  $ax$  and  $by$  in the  $x$ - and  $y$ -direction, respectively. The unifrom magnetic field  $B = [0, 0, B_0]$  and velocity field  $V = [u, v]$  are employed with the Cartesian coordinates  $(x, y)$ .

With the help of the following equations, the dynamics of viscous nanofluid flow with transportation of energy be expressed:

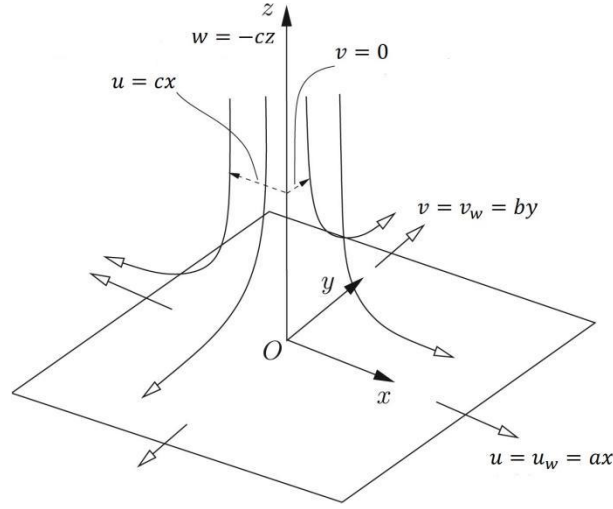


**Figure 4.1:** Flow Diagram

$$\frac{\partial u}{\partial x} + \frac{\partial v}{\partial y} + \frac{\partial w}{\partial z} = 0, \quad (4.1)$$

$$u \frac{\partial u}{\partial x} + v \frac{\partial v}{\partial y} + w \frac{\partial u}{\partial z} + \frac{1}{\rho} \frac{\partial p}{\partial x} = \nu \left[ \frac{\partial^2 u}{\partial x^2} + \frac{\partial^2 u}{\partial y^2} + \frac{\partial^2 u}{\partial z^2} \right] - \frac{\sigma B_0^2 u}{\rho}, \quad (4.2)$$

$$u \frac{\partial v}{\partial x} + v \frac{\partial v}{\partial y} + w \frac{\partial v}{\partial z} + \frac{1}{\rho} \frac{\partial \tilde{p}}{\partial y} = \nu \left[ \frac{\partial^2 v}{\partial x^2} + \frac{\partial^2 v}{\partial y^2} + \frac{\partial^2 v}{\partial z^2} \right] - \frac{\sigma B_0^2 v}{\rho}, \quad (4.3)$$

$$u \frac{\partial w}{\partial x} + v \frac{\partial w}{\partial y} + w \frac{\partial w}{\partial z} + \frac{1}{\rho} \frac{\partial p}{\partial z} = \nu \left[ \frac{\partial^2 w}{\partial x^2} + \frac{\partial^2 w}{\partial y^2} + \frac{\partial^2 w}{\partial z^2} \right], \quad (4.4)$$

$$u \frac{\partial T}{\partial x} + v \frac{\partial T}{\partial y} + w \frac{\partial T}{\partial z} - \alpha_1 \left[ \frac{\partial^2 T}{\partial x^2} + \frac{\partial^2 T}{\partial y^2} + \frac{\partial^2 T}{\partial z^2} \right] = 0, \quad (4.5)$$

$$u \frac{\partial C}{\partial x} + v \frac{\partial C}{\partial y} + w \frac{\partial C}{\partial z} - D_B \left[ \frac{\partial^2 C}{\partial x^2} + \frac{\partial^2 C}{\partial y^2} + \frac{\partial^2 C}{\partial z^2} \right] = 0, \quad (4.6)$$

The parameters in above equations are defined as:

$p$  the pressure, kinematic viscosity is represented by  $\nu$ , the electric conductivity is  $\sigma$ ,  $\alpha_1 \left( = \frac{k}{\rho c_p} \right)$  is heat diffusivity of nanofluid. Where  $k$  is the heat conductivity of fluid,  $\rho$  the density of fluid,  $c_p$  the heat capacity, The heat capacity of nanoparticles for the base fluid is represented by  $\tau$ ,  $(D_T, D_B)$  are called coefficients of thermophoresis and Brownian diffusion, respectively. Moreover, the temperature and concentration at free stream are symbolized as  $(T_\infty, C_\infty)$ . The Hiemenz stagnation-point flow of a viscous fluid is described by the following equations far from its surface with strain rate  $c$ .

$$u = cx, v = 0, w = -cx. \quad (4.7)$$

The sheet extending in both directions, therefore the following surface conditions for the flow field are maintained

$$u = u_w = ax, v = v_w = by, w = 0 \text{ at } z = 0. \quad (4.8)$$

The following boundary criteria are taken into account while analyzing temperature and concentration distributions:

$$T = T_w, C = C_w \text{ at } z = 0, T \rightarrow T_\infty, C \rightarrow C_\infty \text{ as } z \rightarrow \infty. \quad (4.9)$$

Following are the substitution for equations

$$u = cx f'(\eta), v = cy g'(\eta), w = -\sqrt{cv}(f + g), \eta = z \sqrt{\frac{c}{\nu}}, \phi(\eta) = \frac{C - C_\infty}{C_w - C_\infty}, \theta(\eta) = \frac{T - T_\infty}{T_w - T_\infty} \quad (4.10)$$

$$f''' + (f + g)f'' - f'^2 - M^2(f' - 1) + 1 = 0, \quad (4.11)$$

$$g''' + (f + g)g'' - g'^2 - M^2g' = 0, \quad (4.12)$$

$$\theta'' + \text{Pr}(f + g)\theta' + \text{Pr}(N_b\theta'\phi' + N_t\theta'^2) = 0, \quad (4.13)$$

$$\phi'' + \text{LePr}(f + g)\phi' + \frac{N_t}{N_b} \text{LePr}\theta'' = 0, \quad (4.14)$$



and the boundary conditions are:

$$\left. \begin{aligned} f(0) = 0, g(0) = 0, f'(0) = \alpha, g'(0) = \beta, \theta(0) = 1, \phi(0) = 1, \\ f'(\infty) = 1, g'(\infty) = 0, \theta(\infty) = 0, \phi(\infty) = 0. \end{aligned} \right\} \quad (4.15)$$

Where  $\alpha(= \frac{a}{c})$  and  $\beta(= \frac{b}{c})$  are the stretching parameters in streamwise and crossstream direction, Additionally,  $M(= \sqrt{\frac{\sigma B_0^2}{\rho c}})$  is magnetic parameter,  $N_b(= \frac{TD_B(C_w - C_\infty)}{v})$  is Brownian diffusion coefficient,  $N_t(= \frac{TD_T(T_w - T_\infty)}{vT_\infty})$  is thermophoresis parameter,  $Pr(= \frac{v}{\alpha_1})$  is Prandtl number and  $Le(= \frac{\alpha_1}{D_B})$  is Lewis number.

### 4.3 Numerical Problem

Utilizing MATLAB's integrated bvp4c technique, the equations (4.11–4.14) provide the governing ordinary differential equations for the flow rate of a viscous fluid with thermal and entire energy transport, and they are numerically determined. In order to use the BVPC function, the supplied ordinary differential equations were first converted into a system of a first-order ordinary differential equations using the following set of variables.

$$f = y_1, f' = y_2, f'' = y_3, f''' = yy_1 \quad (4.16)$$

$$g = y_4, g' = y_5, g'' = y_6, g''' = yy_2 \quad (4.17)$$

$$\theta = y_7, \theta' = y_8, \theta'' = yy_3 \quad (4.18)$$

$$\phi = y_9, \phi' = y_{10}, \phi'' = yy_4 \quad (4.19)$$

The resulting first order ODEs are

$$yy_1 = -(y_1 + y_4)y_3 + y_2^2 + M^2(y_2 - 1) - 1, \quad (4.20)$$

$$yy_2 = -((y_1 + y_4)y_6) + y_5^2 + M^2y_5, \quad (4.21)$$

$$yy_3 = -Pr(y_1 + y_4)y_8 + PrN_b y_8 y_{10} - PrN_t y_8^2, \quad (4.22)$$

$$yy_4 = -Pr(y_1 + y_4)y_{10} - LePr \frac{N_t}{N_b} yy_3, \quad (4.23)$$

Boundary conditions are

$$\left. \begin{aligned} y_1(0) = 0, y_2(0) = \alpha, y_2(\infty) = 1 \\ y_4(0) = 0, y_5(0) = \beta, y_5(\infty) = 1. \end{aligned} \right\} \quad (4.24)$$

#### 4.4 Discussion of result

The outcomes for the flow field, temperature, and concentration distributions within a viscous nanofluid's Hiemenz stagnation-point MHD flow are shown visually. As a result, a thorough physical justification for these results is given in this part of the study. Throughout all computation of the numerical results, the values of the controlling undefined physical parameters are set at  $\alpha = \beta = 0.5, M = 1, N_t = N_b = 0.5, Pr = Le = 6.5$ . According to Weidman [9], the numerical results of the current investigation can also only be found for a limited range of streamwise stretching  $2 \leq \alpha \leq 2$ .

Figures 4.2(a –c) shows how a magnetic parameter affects the field of movement when a sheet is stretched in a stream-like manner by comparing Figures  $\alpha < 1$  and  $\alpha > 1$ . It should be noticed that the increased trend in  $M$  an increase in the Lorentz forces causes the flow field's cross-stream and vertical directions to drastically diminish. For increase values of  $M$  in the case of the streamwise velocity component, an intriguing outcome is observed. As for  $\alpha < 1$ , the surface stretching rate of strain is greater than the flowing stream's frictionless flow strain rate; hence, for  $\alpha < 1$ , the effects of the stretched sheet exponentially penetrate the free stream having an increasing trend in the  $x$  –direction. On the other hand,  $\alpha > 1$  demonstrates adverse behaviours. In this region, the velocity field becomes free stream.

The centre line in Figure 4.2(a) for  $\alpha = 1$  looks into the notion that surface stretching is not the reason for fluid motion. Figure 4.3(a,b) shows the impact of the magnetic parameter on the flow field when the sheet is contracting. It has been noted that the  $\alpha$  component of the flow field declines while the  $\beta$  component grows and go near the fluid's free stream velocity. Additionally, the velocity of the fluid is physically negative in some areas close to the plate,

which indicates that the influence of the surface's contraction produces flow in the opposite direction of the  $x$  –direction of strain rate only in these areas.

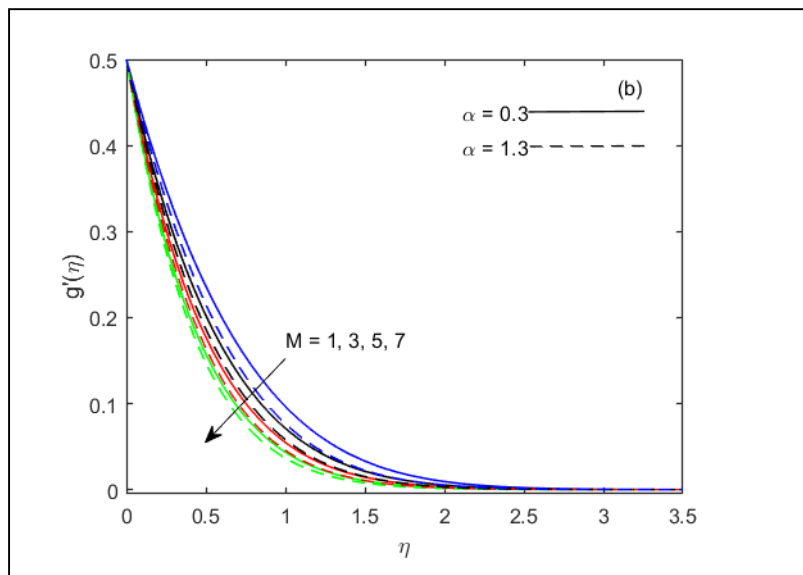
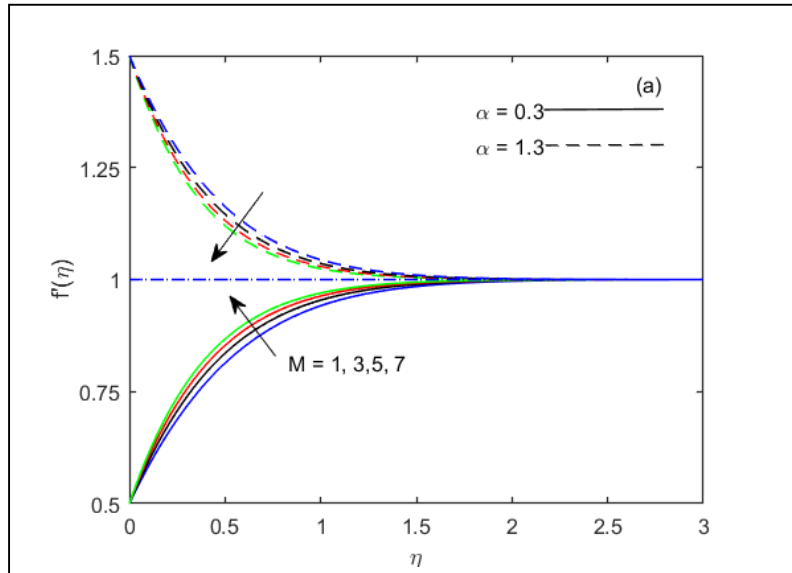
Plots in Figures 4.4(a –c) and 4.5(a,b) investigated the impact of the stretching parameter  $\beta$  regarding the velocity field for sheet stretching and shrinking. The findings demonstrate that the velocity increases in the cross-stream and upward directions as increases. Yet, the outcomes for  $\beta$  and  $M$  are equivalent for the streamwise component of the velocity field. Physically, increasing magnitude of  $\beta$  causes the surface that opposes streamwise flow caused by  $x$  –direction flow rate to stretch out across the stream more. The velocity field is strengthened whenever the  $\beta$  sheet shrinking. However, the reverse flow also generates close to the plate. Figure 4.6(a,b) present the result for the concentration and temperature distribution in Hiemenz flow when the sheet is stretched and contracted As the sheet stretches and shrinks, a paradoxical tendency in the distribution of heat and fluid energy occurs.. Higher rates of thermal and kinetic energy are present when a sheet is stretching.

Figure 4.7(a,b) report the significance of the Brownian motion and thermophoresis processes of nanoparticles under viscous fluids for both concentration and temperature distributions. The significant thermal gradient in the fluid causes the thermophoretic parameter to increase heat and mass movement. Because a strong thermal gradient increases the drift velocity of base liquid molecules as well as nanoparticles, the concentration field and temperature rise as a result of this. Due to the Brownian movement parameter, the temperature field expands whereas the concentration field contracts. Physical barriers to mass transmission are created by the Brownian motion of the nanoparticles, which also elevates the temperature of a nanofluid. The outcome is a drop in the concentration field and an increase in the temperature field.

Figure 4.8(a,b) provides the streamwise and cross-stream wall shear stress parameters. As a magnetic parameter  $M$  increases, these parameters also increase. Additionally It should be emphasised that whereas streamwise surface shear stress is uniform over the entire domain, cross-stream shear stress employing algebra decays between zero and the negative direction.. The accuracy of the current investigation was ensured by the findings in Fig. 4.8(a), which match those reported by Weidman. [9] Table 1 gives numerical estimates for different amounts of relevant parameters for mass and thermal transfer rates while Hiemenz flow across a sheet's surface.

From tabular data, it can be deduced that streamwise stretching and a strong Lorentz force

increase the rate of heat transfer.



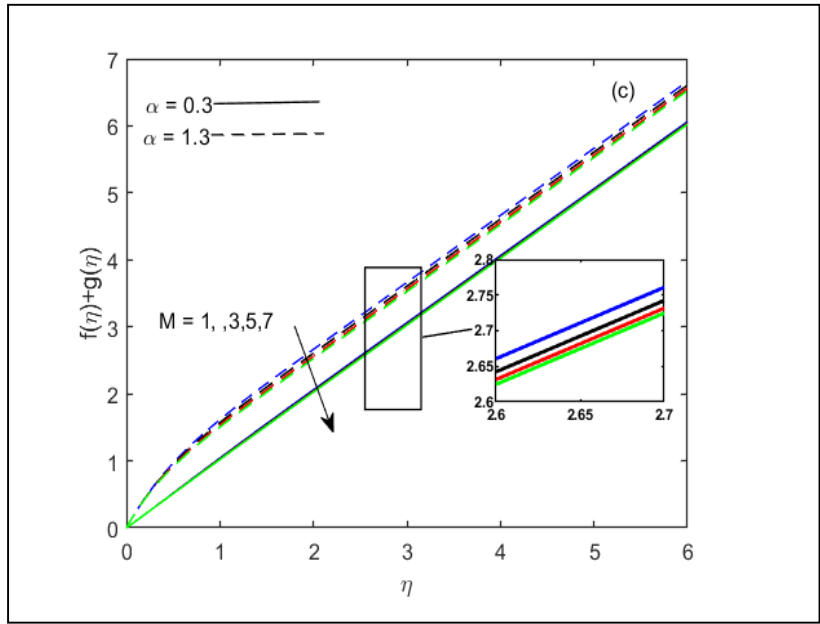
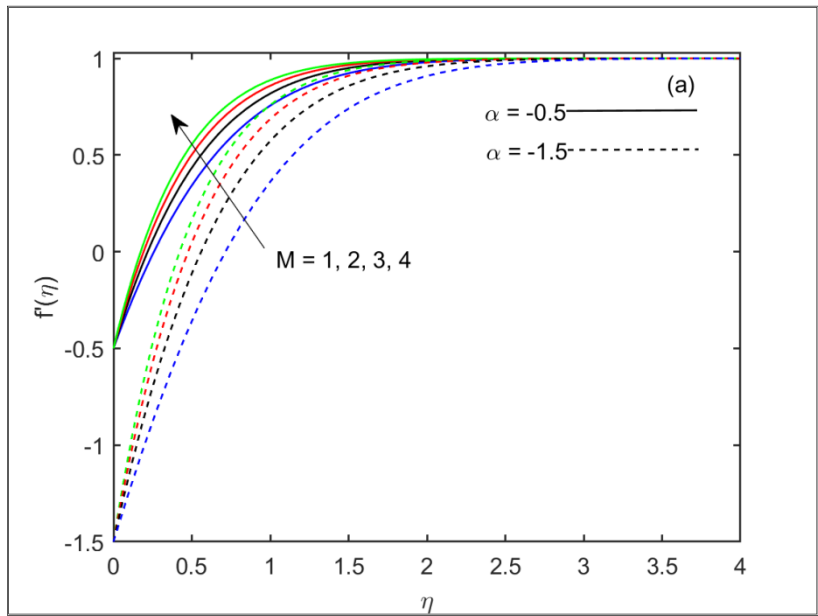


Figure 4.2 (a-c): Impact of M on flow field (stretching).



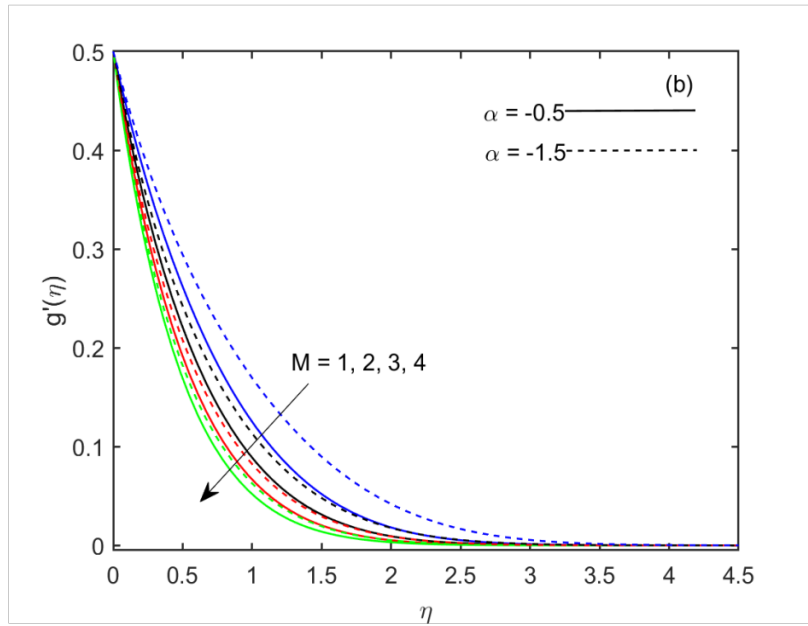
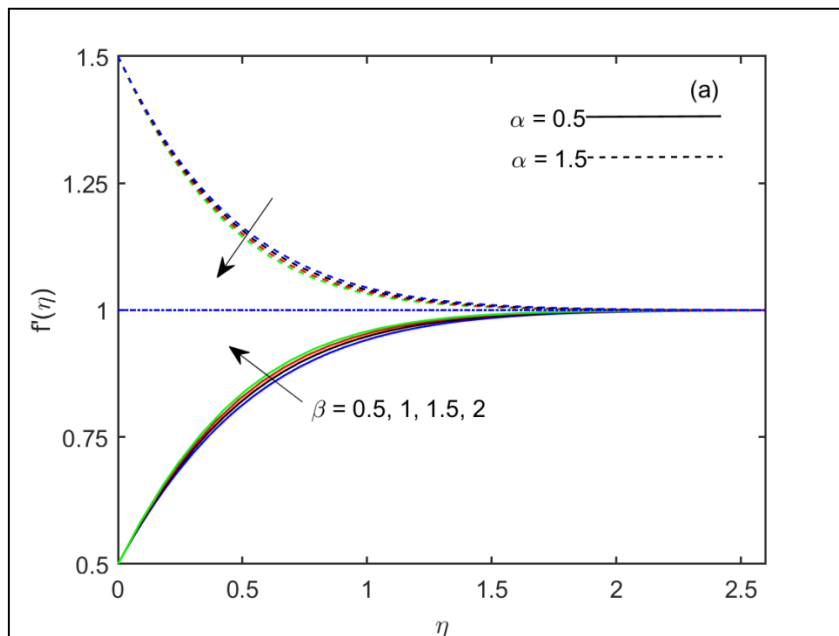


Figure 4.3 (a,b): Impact of M on flow field (Shrinking).



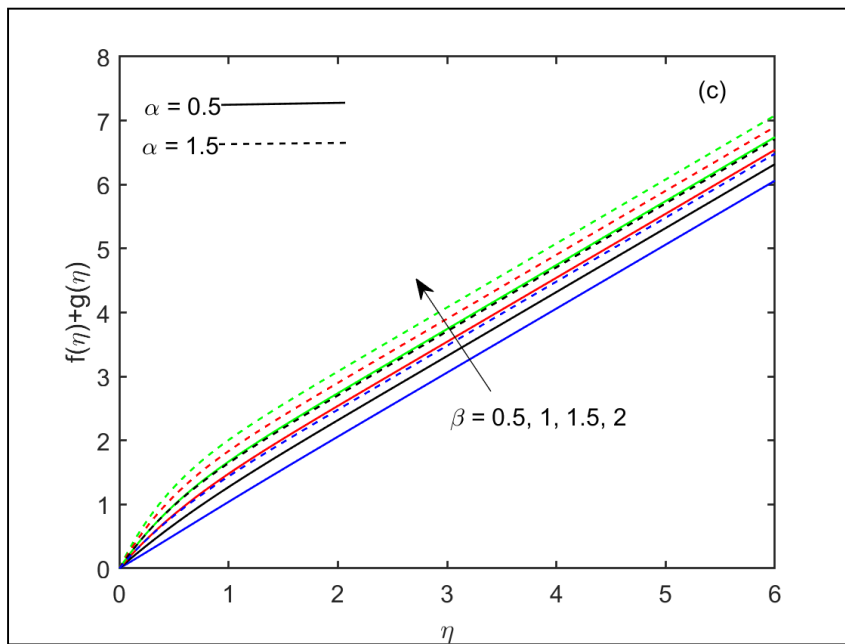
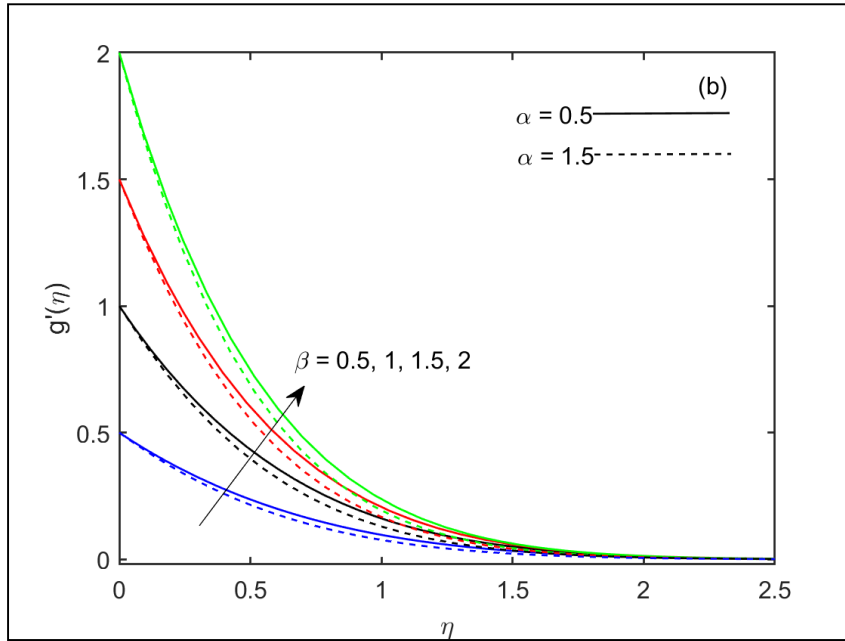


Figure4. 4(a-c): Impact of  $\beta$  on flow field (Stretching).

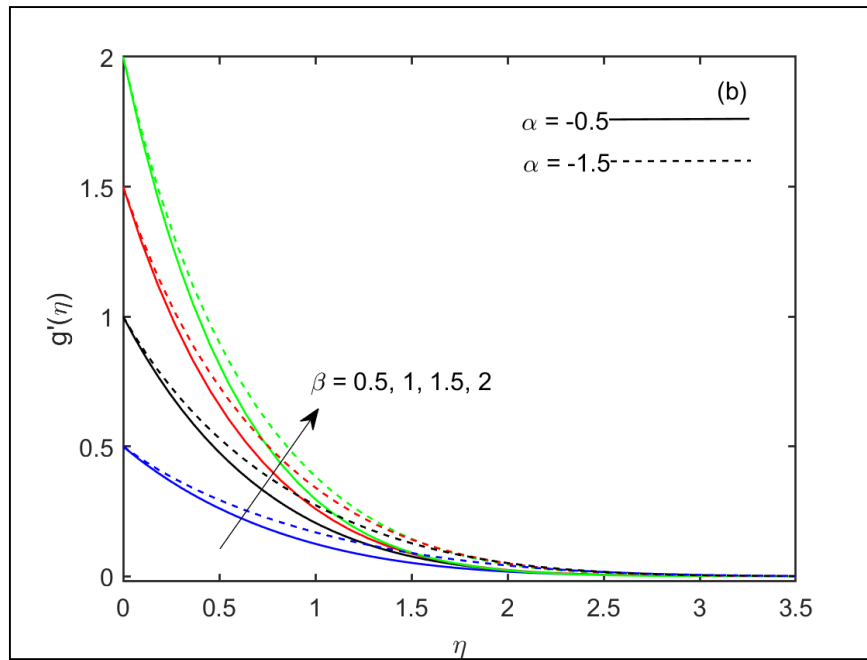
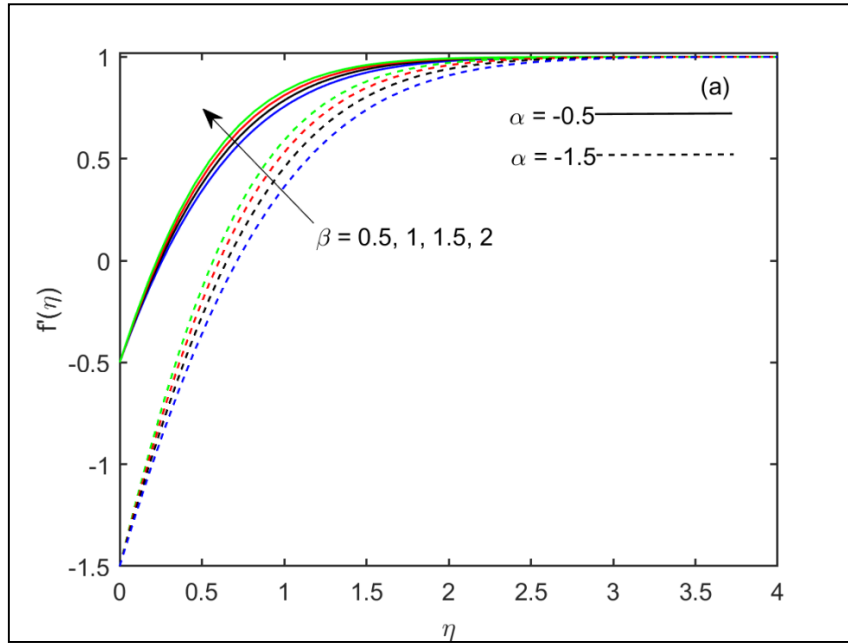


Figure 4.5(a,b): Impact of  $\beta$  on flow field (Shrinking).



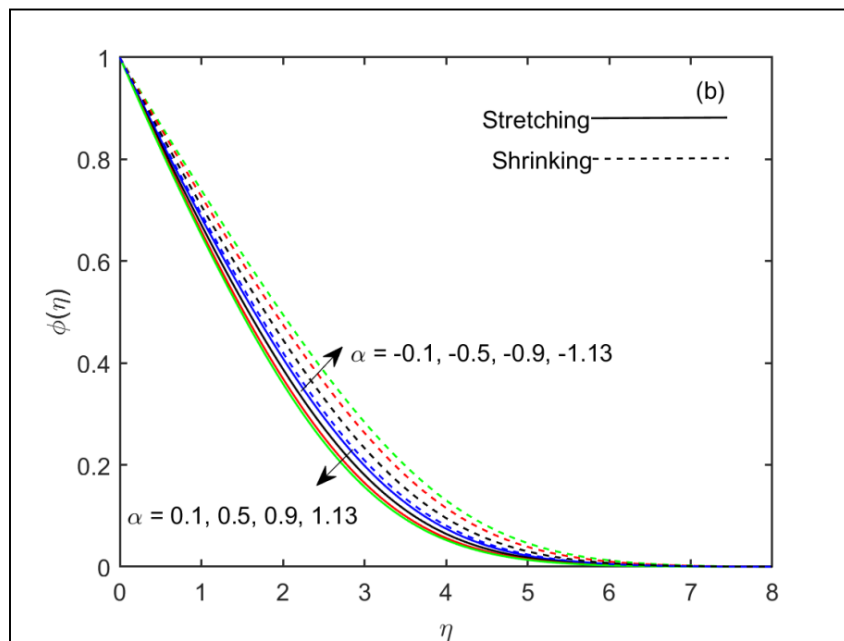
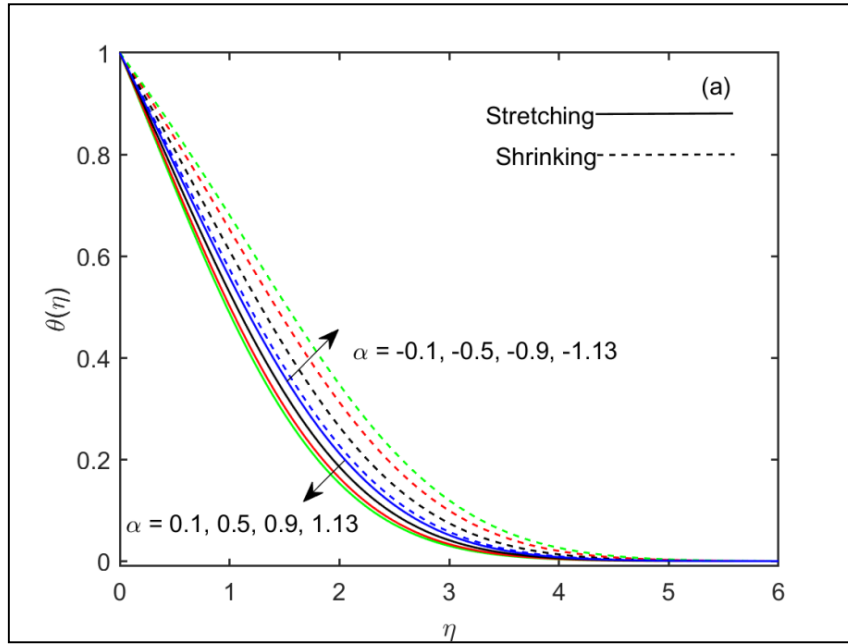


Figure 4.6 (a,b): Impact of  $\alpha$  on temperature and concentration field.

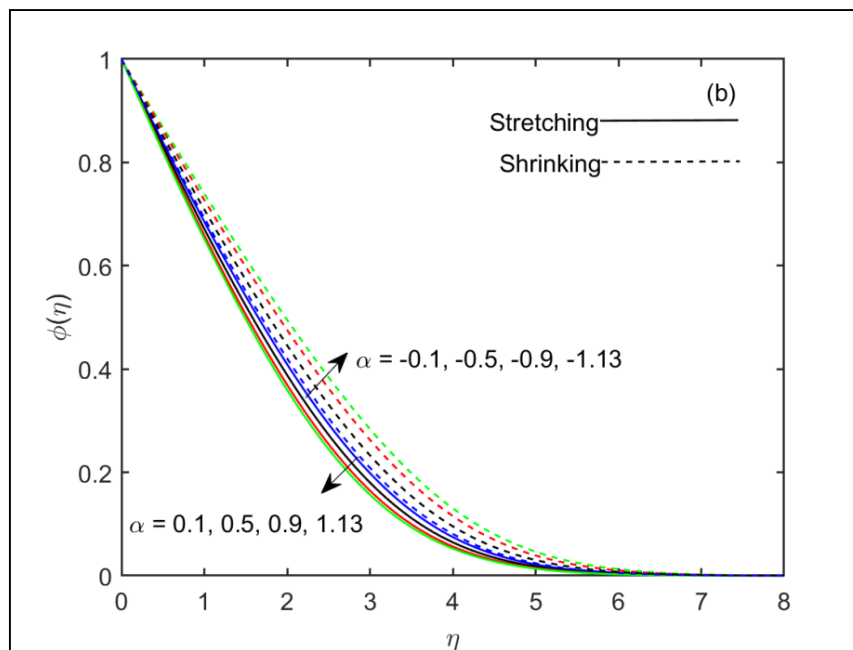
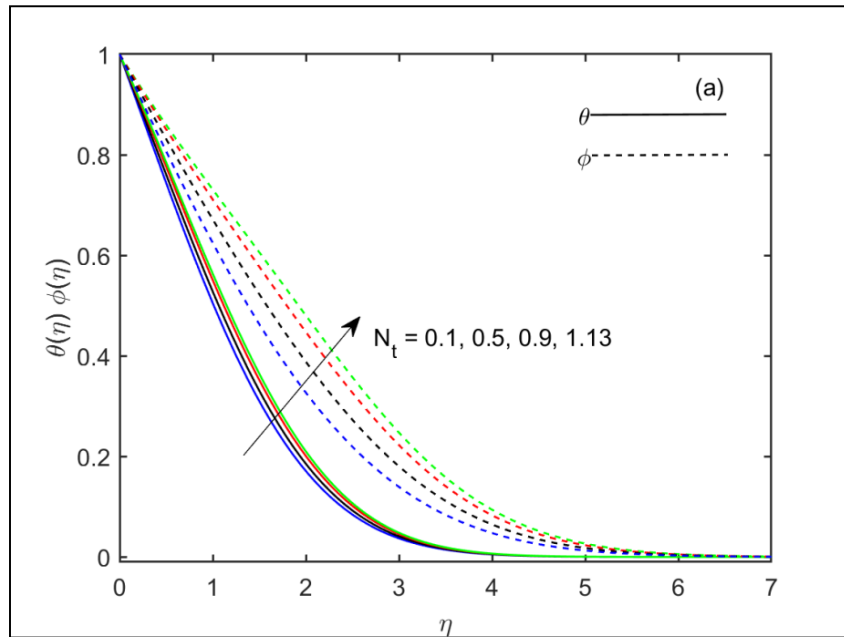


Figure 4.7(a,b): Impact of  $N_t$  and  $N_b$  on temperature and concentration field.

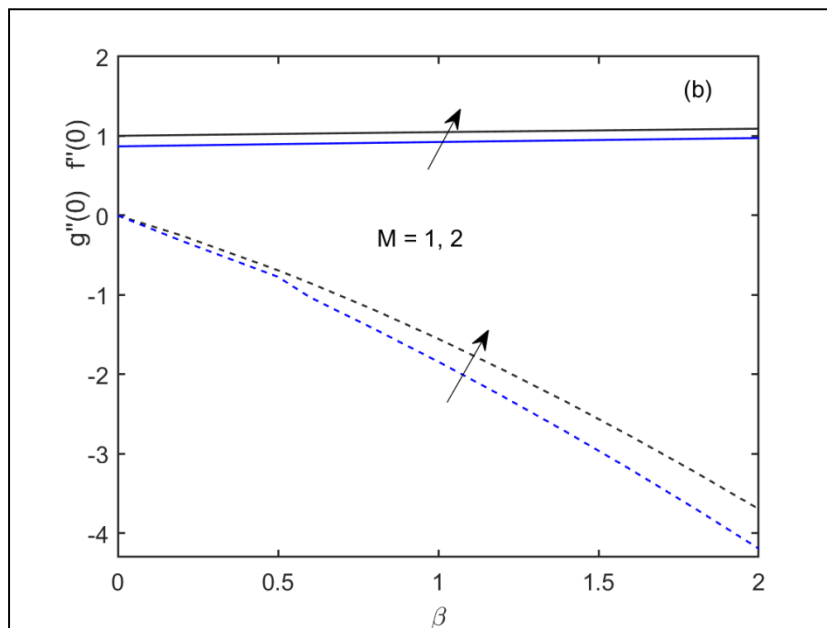
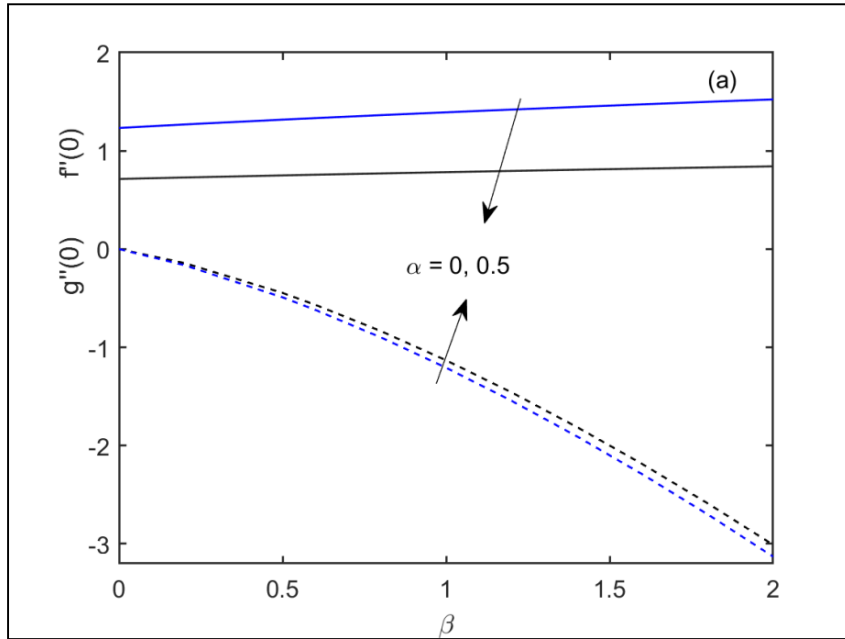


Figure 4.8 (a,b): Impact of  $\alpha$  and  $M$  on stress parameters  $\{f''(0), g''(0)\}$ .

## CHAPTER 5

### Flow of hybrid nanofluid in Hiemenz's phenomenon over stretchable surface

#### 5.1 Introduction

In this chapter, steady flow of nanofluid and hybrid nanoparticles (SWCNT, MWCNT with a base fluid water) are studied under the presence of MHD. It is investigated how a viscous hybrid nanofluid flow over a stretchable sheet that can stretch in two directions. In this work, the Xue model for the hybrid nanofluid is used to examine the behaviour of solute & thermal energy transit in three-dimensional in Hiemenz flow of the nanofluid under the influence of the magnetic field. The bvp4c technique is used to numerically solve the equations that are generated, and the variation in the physical parameters for velocity and temperature are visualized graphically. The better performance of hybrid nanofluid is demonstrate through a graphical comparison of basefluid, nanofluid (SWCNT and water) and hybrid nanofluid (SWCNT, MWCNT and water).

#### 5.2 Mathematical formulation

Thermal transmission is investigated in a steady and magneto hydrodynamic flow containing hybrid nanofluid (MWCNT-SWCNT with water) towards a stretched sheet. The sheet lies in  $z = 0$  and the the sheet is linearly stretching in  $xy - plane$  with rates  $a$  and  $b$ , respectively. The temperature of the surface of the sheet is assumed as constant. The behaviour of a viscous hybrid nanofluid flow with energy transfer can be represented using the following equations.

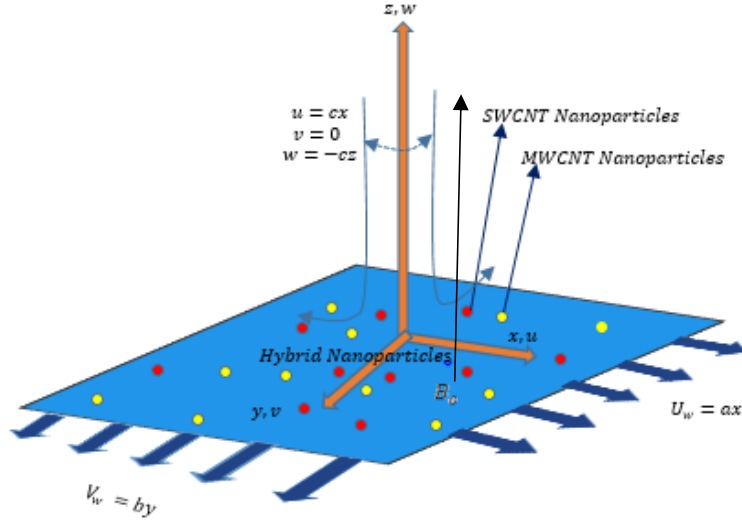


**Figure 5.1:** Geometry of the problem.

The following are the governing equations that is modified for the present study.

$$\frac{\partial u}{\partial x} + \frac{\partial v}{\partial y} + \frac{\partial w}{\partial z} = 0, \quad (5.1)$$

$$u \frac{\partial u}{\partial x} + v \frac{\partial v}{\partial y} + w \frac{\partial w}{\partial z} + \frac{1}{\rho_{hnf}} \frac{\partial p}{\partial x} = \frac{\mu_{hnf}}{\rho_{hnf}} \left[ \frac{\partial^2 u}{\partial x^2} + \frac{\partial^2 u}{\partial y^2} + \frac{\partial^2 u}{\partial z^2} \right] - \frac{\sigma B_0^2 u}{\rho_{hnf}}, \quad (5.2)$$

$$u \frac{\partial v}{\partial x} + v \frac{\partial v}{\partial y} + w \frac{\partial v}{\partial z} + \frac{1}{\rho_{hnf}} \frac{\partial p}{\partial y} = \frac{\mu_{hnf}}{\rho_{hnf}} \left[ \frac{\partial^2 v}{\partial x^2} + \frac{\partial^2 v}{\partial y^2} + \frac{\partial^2 v}{\partial z^2} \right] - \frac{\sigma B_0^2 v}{\rho_{hnf}}, \quad (5.3)$$

$$u \frac{\partial w}{\partial x} + v \frac{\partial w}{\partial y} + w \frac{\partial w}{\partial z} + \frac{1}{\rho_{hnf}} \frac{\partial p}{\partial z} = \frac{\mu_{hnf}}{\rho_{hnf}} \left[ \frac{\partial^2 w}{\partial x^2} + \frac{\partial^2 w}{\partial y^2} + \frac{\partial^2 w}{\partial z^2} \right], \quad (5.4)$$

$$u \frac{\partial T}{\partial x} + v \frac{\partial T}{\partial y} + w \frac{\partial T}{\partial z} = \frac{k_f}{(\rho_{cp})_f} \left[ \frac{\partial^2 T}{\partial x^2} + \frac{\partial^2 T}{\partial y^2} + \frac{\partial^2 T}{\partial z^2} \right], \quad (5.5)$$

The parameters in above equations are defined as:

$p$  the pressure, kinematic viscosity is denoted by  $\nu$ , electric conductivity is represented by  $\sigma$ ,

$\alpha_1 \left( = \frac{k}{\rho c_p} \right)$  is heat diffusivity of nanofluid where,  $k$  represents heat conductivity of fluid,  $\rho$  the density of fluid,  $c_p$  the heat capacity,  $\tau$  is the symbol used for heat capacity of nanoparticles to the base fluid. Moreover, the temperature and concentration at free stream are symbolized as  $(T_\infty, C_\infty)$ . The following equations describe that far away from the surface along strain rate the behavior of Hiemenz stagnation-point flow of viscous fluid.

$$u = cx, \quad v = 0, \quad w = -cx \text{ at } z \rightarrow \infty. \quad (5.6)$$

The sheet is also permeable when extending in both directions, therefore the following surface conditions for the flow field are maintained

$$u = u_w = ax, \quad v = v_w = by, \quad w = 0 \text{ at } z = 0. \quad (5.7)$$

The following boundary criteria are taken into account while analysing temperature and concentration distributions:

$$T = T_w, \text{ at } z = 0, \quad T \rightarrow T_\infty, \text{ as } z \rightarrow \infty. \quad (5.8)$$

$$u = cx f'(\eta), \quad v = cy g'(\eta), \quad w = -\sqrt{cv_f}(f + g), \quad \eta = z \sqrt{\frac{c}{v_f}}, \quad \theta(\eta) = \frac{T - T_\infty}{T_w - T_\infty}. \quad (5.9)$$

Following ordinary equations are given below

$$\frac{A_1}{A_2} f'''(\eta) + f''(\eta)(f + g) - f'^2(\eta) - M^2 (f'(\eta) - 1) + 1 = 0, \quad (5.10)$$

$$\frac{A_1}{A_2} g'''(\eta) + g''(\eta)(f + g) - g'^2(\eta) - M^2 g'(\eta) = 0, \quad (5.11)$$

$$\frac{A_5 A_4}{A_3} \theta'' + \text{Pr} \theta'(f + g) = 0, \quad (5.12)$$

With the boundary conditions

$$\left. \begin{aligned} f(0) = 0, \quad g(0) = 0, \quad f'(0) = \alpha, \quad g'(0) = \beta, \quad \theta(0) = 1, \\ f'(\infty) = 1, \quad g'(\infty) = 0, \quad \theta(\infty) = 0. \end{aligned} \right\} \quad (5.13)$$

Here  $f, g$  are velocity profile,  $\theta$  is temperature and  $M(= \sqrt{\frac{\sigma B_0^2}{\rho c}})$  is magnetic parameter,  $Pr(= \frac{v}{\alpha})$  is Prandtl number.  $A_1 A_2 A_3 A_4 A_5$  is expressed as ;

$$\text{where, } \left. \begin{aligned} A_1 &= \frac{\mu_{hnf}}{\mu_f}, A_2 = \frac{\rho_{hnf}}{\rho_f}, A_3 = \frac{(\rho_{cp})_{hnf}}{(\rho_{cp})_f}, A_4 = \frac{K_{hnf}}{K_{bf}}, A_5 = \frac{K_{bsf}}{K_f}, Pr = \frac{v}{\alpha}, \\ \alpha &= \frac{K_f}{(\rho_{cp})_f} \end{aligned} \right\} (5.14)$$

### 5.3 Numerical solution

The governing ordinary differential equations for the flow of a viscous fluid containing thermal as well as total energy transfer are given in Eqs (5.10-5.12), and are numerically determined with MATLAB's integrated bvp4c function. To apply the BVPC function, the given ordinary differential equations were first transformed into a system of first-order ODE's utilizing a following set of variables.

Conversion of ODE's into system of first order ODE's

$$f = y_1, f' = y_2, f'' = y_3, f''' = yy_1, \quad (5.15)$$

$$g = y_4, g' = y_5, g'' = y_6, g''' = yy_2, \quad (5.16)$$

$$\theta = y_7, \theta' = y_8, \theta'' = yy_3, \quad (5.17)$$

Resulting first order ODEs are:

$$yy_1 = -(y_1 + y_4)y_3 + y_2^2 + M^2(y_2 - 1) - 1) \frac{A_1}{A_2}, \quad (5.18)$$

$$yy_2 = -(y_1 + y_4)y_6 + y_5^2 + M^2y_5) \frac{A_2}{A_1}, \quad (5.19)$$

$$yy_3 = (-Pr y_8(y_1 + y_4)) \frac{A_3}{A_4 A_5}, \quad (5.20)$$

The corresponding BCs with these mentioned first order differential systems are

$$\left. \begin{aligned} (y_1(0) = 0, y_2(0) = \alpha, y_2(\infty) = 1) \\ (y_4(0) = 0, y_5(0) = \beta, y_5(\infty) = 1.) \end{aligned} \right\} \quad (5.21)$$

**Table 5.1.** The thermophysical characteristics of the analyzed nanofluids. [71]

Physical Properties	Nanofluid
Dynamic viscosity	$\mu_{nf} = \mu_f(1 - \phi)^{-\frac{5}{2}},$
Density	$\rho_{nf} = \phi\rho_{SWCNT} + (1 - \phi)\rho_f,$
Heat capacity	$(\rho c_p)_{nf} = \phi(\rho c_p)_{SWCNT} + (1 - \phi)(\rho c_p)_f,$
Thermal conductivity	$\frac{k_{nf}}{k_f} = \frac{(1-\phi)+2\phi\frac{k_{SWCNT}}{k_{SWCNT}-k_f}\ln\left(\frac{k_{SWCNT}+k_f}{k_f}\right)}{(1-\phi)+2\phi\frac{k_f}{k_{SWCNT}-k_f}\ln\left(\frac{k_{SWCNT}+k_f}{k_f}\right)}$

**Table 5.2.** Thermophysical characteristics for the hybrid nanofluids. [71]

Physical Properties	Hybrid
Dynamic viscosity	$\mu_{hnf} = \mu_f(1 - \phi_1)^{-\frac{5}{2}}(1 - \phi_2)^{-\frac{5}{2}},$
Density	$\rho_{hnf} = \phi_2\rho_{SWCNT} + (1 - \phi_2)\{(1 - \phi_1)\rho_f + \phi_1\rho_{MWCNT}\}$
Heat capacity	$(\rho c_p)_{hnf} = \phi_2(\rho c_p)_{SWCNT} + (1 - \phi_2)\{(1 - \phi_1)(\rho c_p)_f + \phi_1(\rho c_p)_{MWCNT}\},$
Thermal conductivity	$\frac{k_{hnf}}{k_{bf}} = \frac{(1-\phi_2)+2\phi_2\frac{k_{SWCNT}}{k_{SWCNT}-k_{bf}}\ln\left(\frac{k_{SWCNT}+k_{bf}}{k_{bf}}\right)}{(1-\phi_2)+2\phi_2\frac{k_{bf}}{k_{SWCNT}-k_{bf}}\ln\left(\frac{k_{SWCNT}+k_{bf}}{k_{bf}}\right)}$ Where,
	$\frac{k_{bf}}{k_f} = \frac{(1-\phi_1)+2\phi_1\frac{k_{MWCNT}}{k_{MWCNT}-k_f}\ln\left(\frac{k_{MWCNT}+k_f}{k_f}\right)}{(1-\phi_1)+2\phi_1\frac{k_f}{k_{MWCNT}-k_f}\ln\left(\frac{k_{MWCNT}+k_f}{k_f}\right)},$



**Table 5.3.** Thermophysical characteristics of base fluid (water) and nanoparticles. [71]

Physical Properties	Water(basefluid)	MWCNT	SWCNT
Heat capacity $C_p(Jkg^{-1}K^{-1})$	4179.00	786	425
Density $\rho(kgm^{-3})$	997.100	1600	2600
Thermal conductivity $K (Wm^{-1}K^{-1})$	0.61300	3000	6600

Where,  $k_f$  is the heat conductivity of the working fluid and, for multiwall carbon nanotubes (MWCNT) and single wall carbon nanotubes (SWCNT) respectively,  $\phi_1$  and  $\phi_2$  are the solid volume fraction. Here, the subscripts  $hnf$  and  $nf$  stand for the thermophysical properties of the hybrid nanofluid and the nanofluid, respectively.

#### 5.4 Presentation result

The velocity components for the higher magnetic parameter values, stretching parameter, and prandtl parameter are shown in figures (5.1-5.9). The results demonstrate that given the magnetic parameter, stretching parameter, and prandtl parameter, the velocity falls exponentially. Figure 5.1 and 5.2 depicts a fall in the magnetic parameter together with a fall in the velocity profile. The impact of the magnetic parameter  $M$  on the velocity distribution. The velocity profile reduces out as the values of magnetic parameter  $M$  rise. The strong magnetic field boosts the Lorentz force, resulting in the resistive force to prevent and slow the fluid's flow. Figure 5.3 and 5.4 depicts the change in velocity profile as the shrinking parameter  $a_1$  is increased. Figure 5.5 and 5.6 depicts the change in velocity profile as the stretching parameter  $b_1$  is increased and decreases for shrinking parameter. Figure 5.5 shows the decline in velocity profile as the shrinking parameter  $b_1$  is increased. The influence of the magnetic parameter, stretching parameter, and prandtl parameter on the temperature profile is depicted in figures. 5.7-5.9. Magnetic, stretching and shrinking parameters increase for velocity profile. The influence of the magnetic parameter, stretching parameter, and prandtl parameter on the temperature profile is depicted in figures. 5.10 to 5.17. Figure 5.10 and 5.11 illustrates the relationship between the temperature profile and the magnetic parameter  $M$ . Magnetic Parameter increases with an increase in temperature. Figure 5.12 and 5.13 illustrates the

relationship between the temperature profile and the stretching parameter and shrinking parameter  $b_1$ . Stretching parameter and shrinking parameter  $b_1$  increases with an increase in temperature. Figure 5.14 and 5.15 illustrates the relationship between the temperature profile and the stretching parameter and shrinking parameter  $a_1$ . Stretching parameter and shrinking parameter  $b_1$  decreases with an increase in temperature.

Figure 5.16 and 5.17 illustrates the relationship between the temperature profile and the Prandtl number  $Pr$ . Figure 5.16 illustrates how the temperature profile changes as the Prandtl number rises. Figure 5.16 shows how the Prandtl number influences the thermal distribution. With a rise in the Prandtl number, temperature is seen to decrease. High  $Pr$  causes the fluid to become more viscous, which decreases temperature since high  $Pr$  decreases the fluid's thermal diffusivity. Figure 5.17 shows the decrease in temperature profile with increase in Prandtl number.

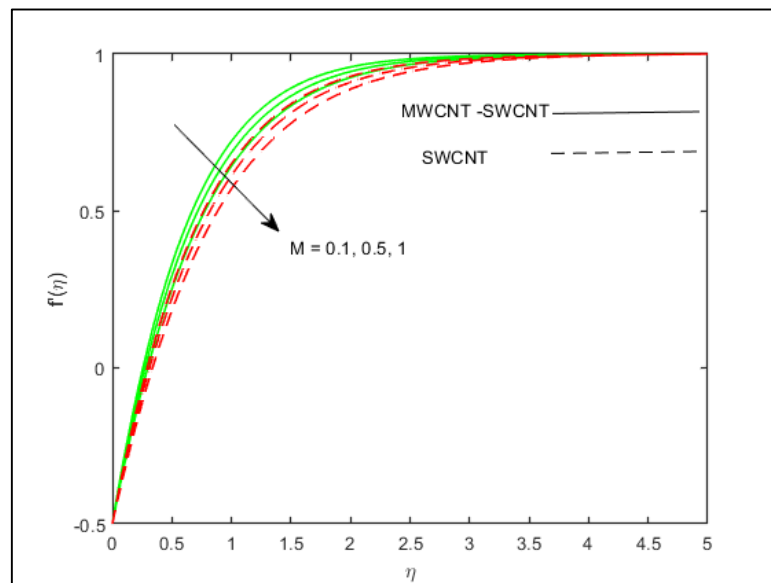


Figure 5.2: influence of  $M$  (stretching) on velocity profile.

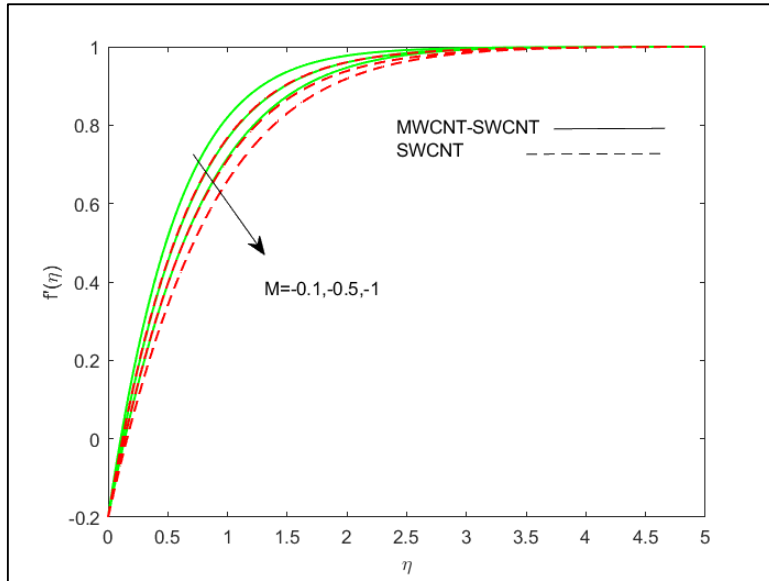


Figure 5.3: influence of  $M$  (shrinking) on velocity field.

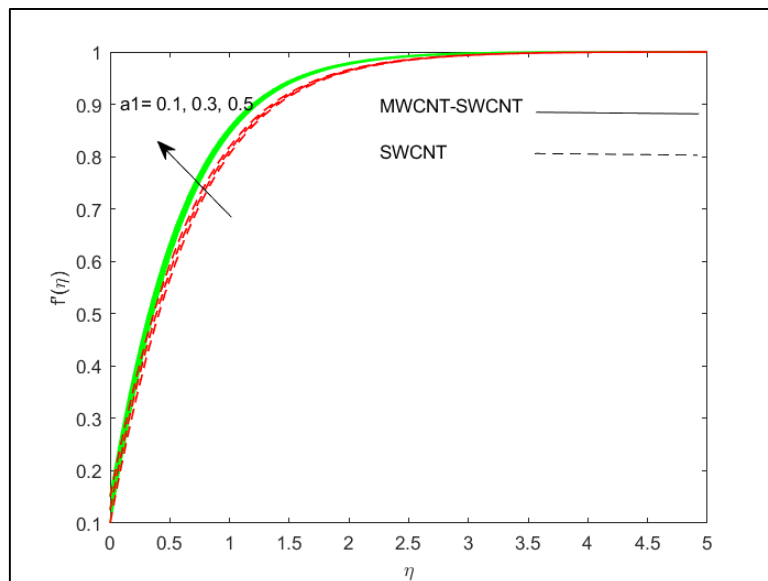


Figure 5.4: influence of  $a_1$  (stretching) on velocity profile.

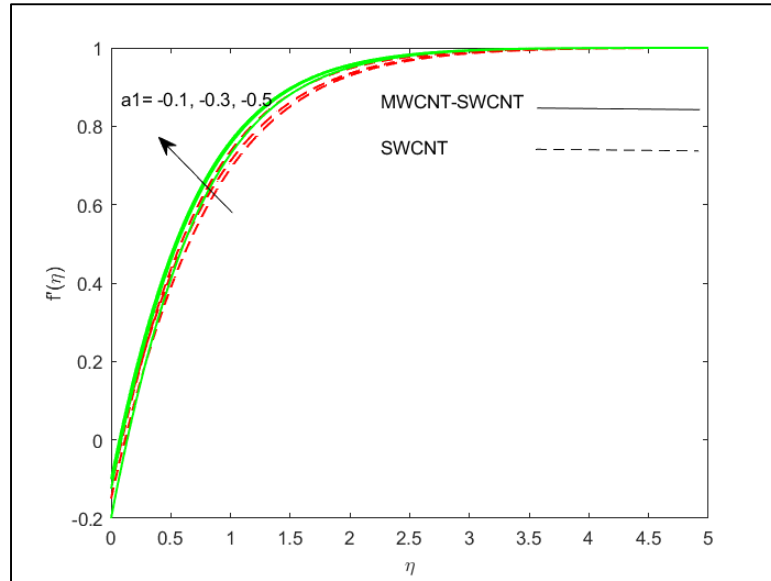


Figure 5.5: influence of  $a_1$  (shrinking) on velocity profile.

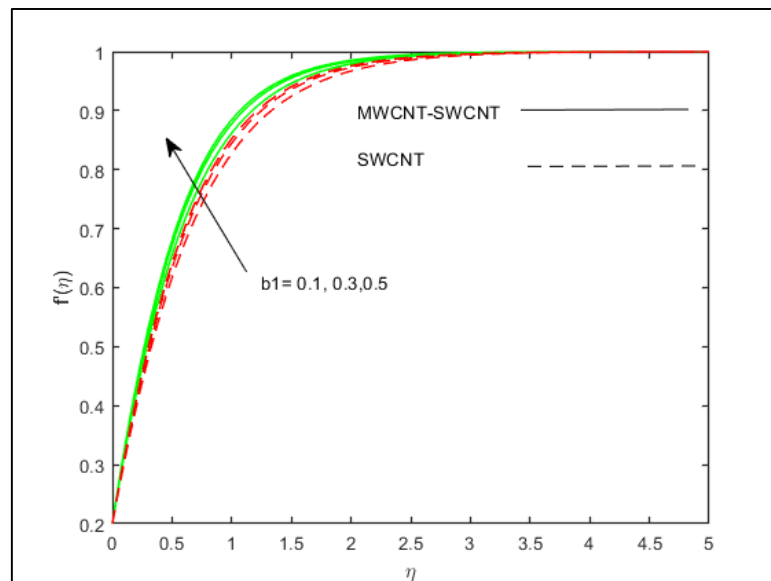


Figure 5.6: influence of  $b_1$  (stretching) on velocity profile.

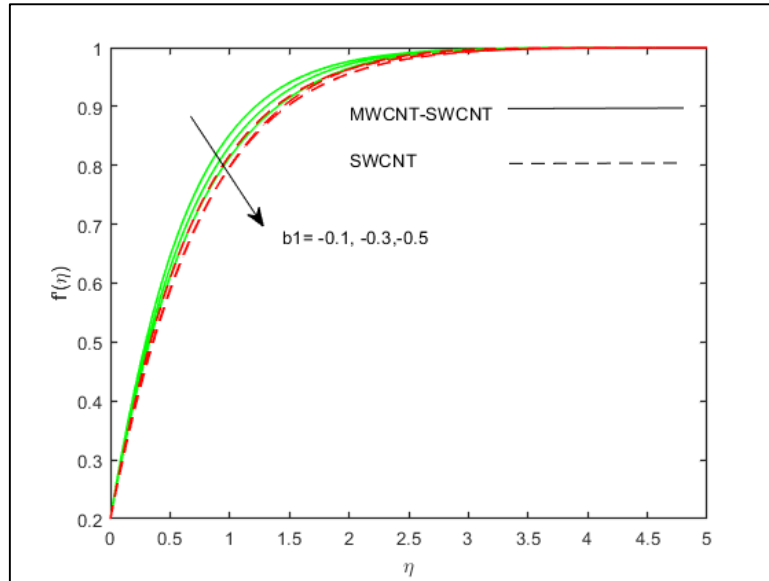


Figure 5.7: influence of  $b_1$  (shrinking) on velocity field.

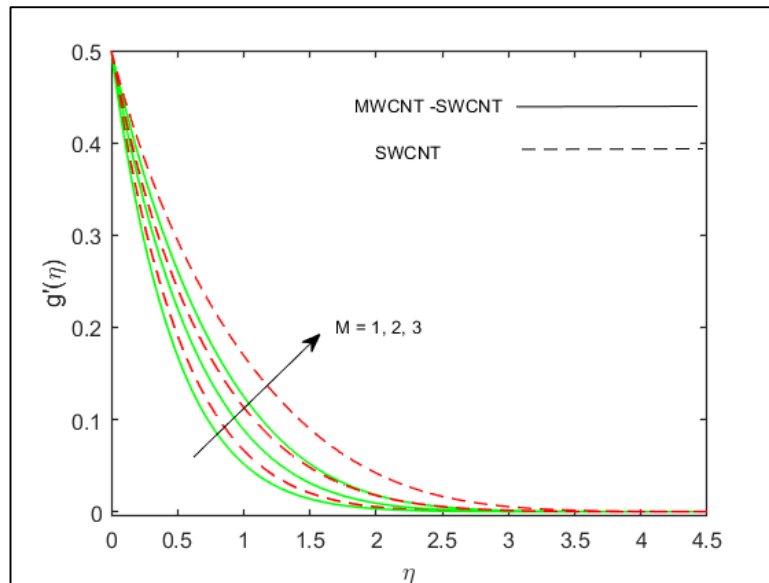


Figure 5.8: Influence of  $M$  (stretching) on velocity field.

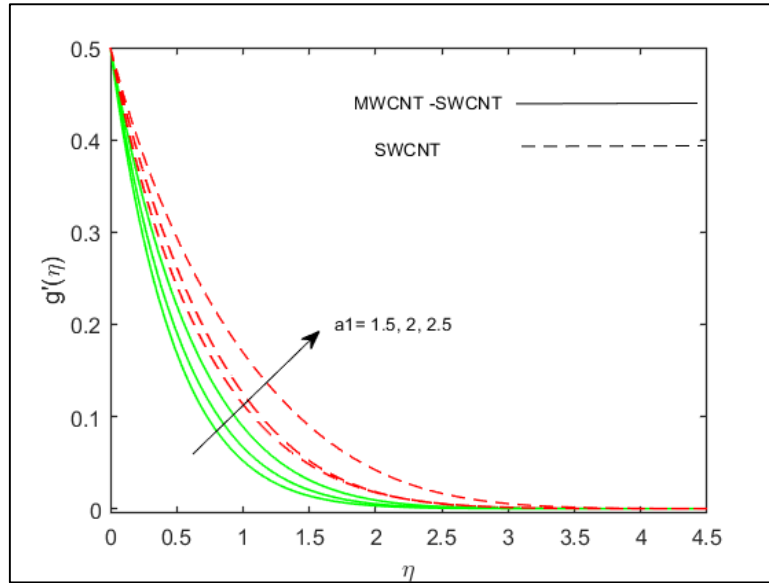


Figure 5.9: Influence of  $a_1$ (stretching) on velocity field.

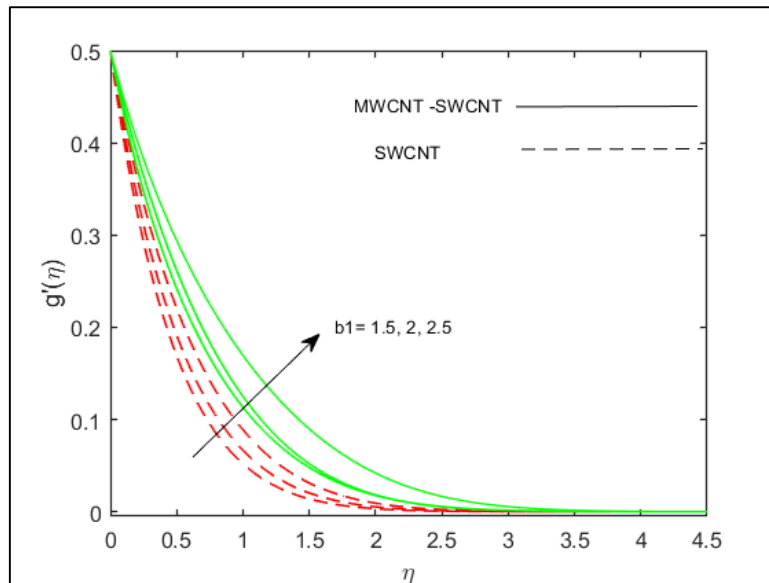


Figure 5.10: influence of  $b_1$ (stretching) on velocity field.

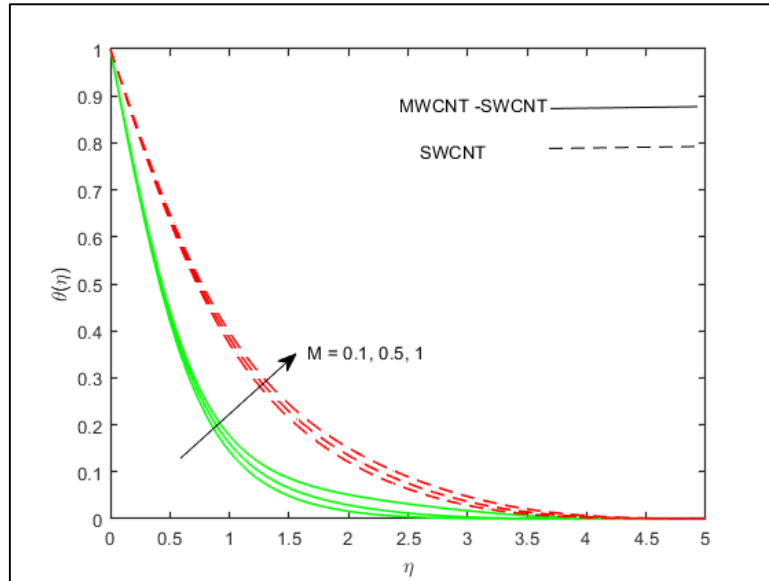


Figure 5.11: Influence of  $M$  (stretching) on temperature profile.

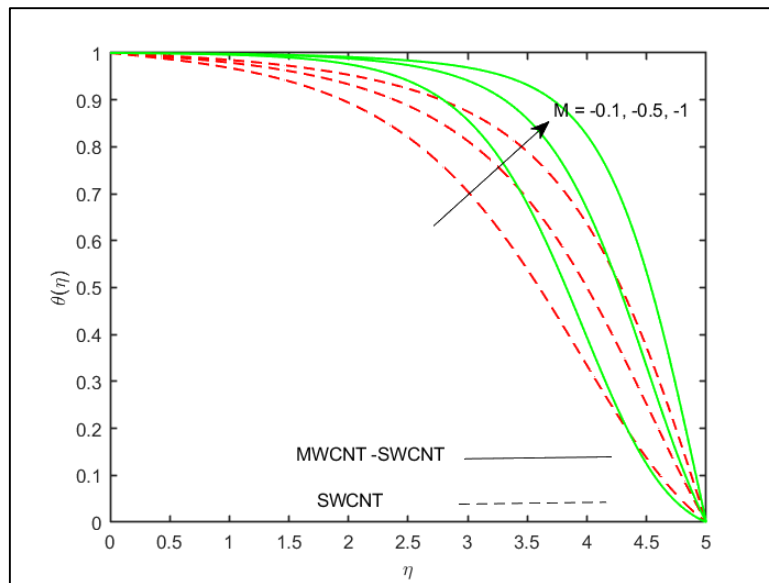


Figure 5.12: influence of  $M$  (shrinking) on temperature profile.

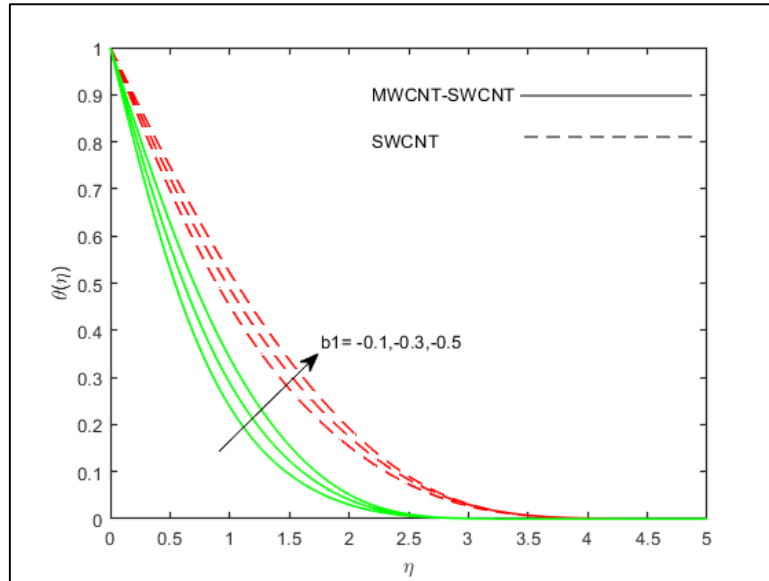


Figure 5.13: Influence of  $b_1$  (shrinking) on temperature profile.

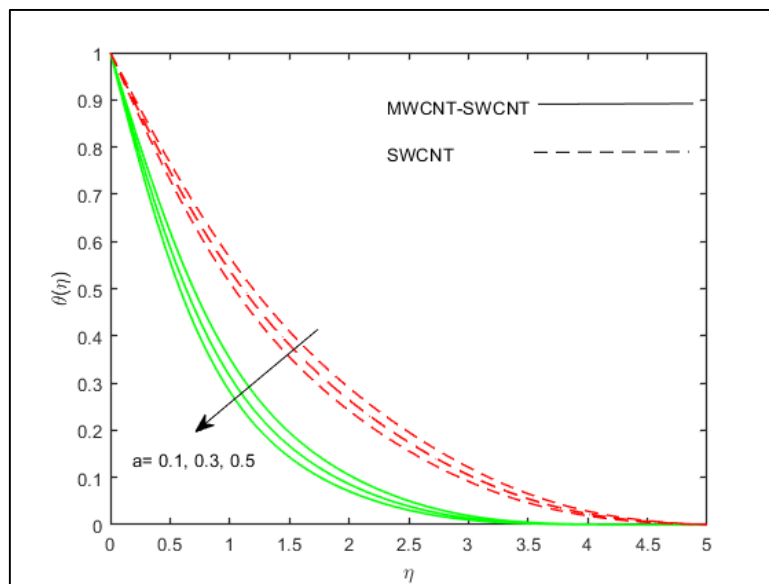


Figure 5.14: Influence of  $a_1$  (stretching) on temperature profile.



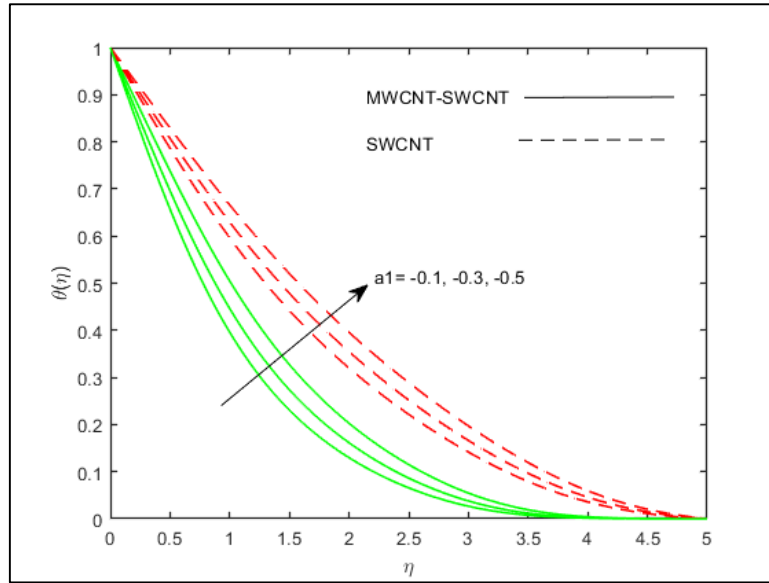


Figure 5.15: Influence of  $a_1$  (shrinking) on temperature profile.

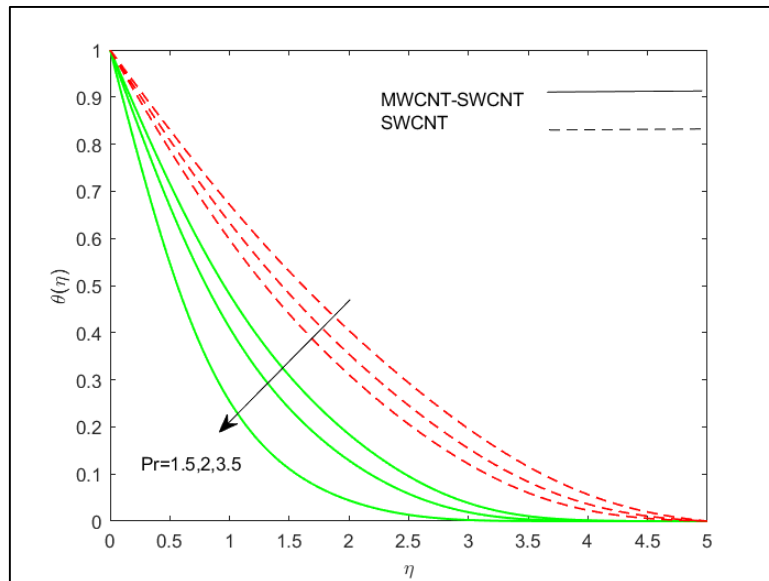


Figure 5.16: influence of  $Pr$  on temperature profile.

## CHAPTER 6

### 6.1 Conclusions

In this research, In the presence of MHD, the flow of a viscous nanofluid along a bi-directional stretching sheet examined near the Hiemenz stagnation point. The phenomena of heat and mass transfer also be addressed. Additionally, the convection process incorporated under the influence of hybrid nanoparticles. The set of equations expressed in terms of PDEs, which was then transformed into ODEs to further simplify them. The numerical analysis of the problem provides the key aspects mentioned below.

A higher  $\beta$  stretching parameter value increased both the cross-stream and vertical flow velocity field. When a sheet was shrinking, the negative velocity might be observed in a specific area near the surface. Due to the random movement and thermo-migration of nanoparticles, the heat and total energy transport was improved during the flow of viscous fluids. With increasing values of  $M$ , the velocity profile decreased. The Lorentz force, that strengthened by a strong magnetic field, amplified by the resistive force and used to stop and slow down fluid movement. Higher values of  $Pr$  reduced the fluid's thermal diffusivity, the fluid become more viscous, which lower temperature. Stretching and shrinking parameter increased the temperature profile significantly. A reduction in temperature was observed with an increasing trend in the prandtl number.

### 6.2 Future work

In this work the effects of heat transfer in Hiemenz flow of viscous nanofluid with hybrid nanofluid towards bi-directional sheet under the influence of MHD have been analyzed. However, there is still space to improve the existing work in order to address other different concerns. The following are some interesting possible studies that could be done in the future. This study can be extended to the MHD flow of a hybrid nanofluid over a curved surface under thermal radiation and Arrhenius activation energy. Various types of mathematical model for hybrid nanofluid can employed in future to investigate the thermal characteristics of viscous nanofluid. This study can also be performed in rotating frame under the magnetic field and buoyancy force effect.

## References

- [1]. Liu, M.S., Lin, M.C.C., Tsai, C.Y. and Wang, C.C., 2006. Enhancement of thermal conductivity with Cu for nanofluids using chemical reduction method. *International Journal of Heat and Mass Transfer*, 49(17-18), pp.3028-3033.
- [2]. Sharma, P., Baek, I.H., Cho, T., Park, S. and Lee, K.B., 2011. Enhancement of thermal conductivity of ethylene glycol-based silver nanofluids. *Powder Technology*, 208(1), pp.7-19.
- [3]. Madhesh, D. and Kalaiselvam, S., 2014. Experimental analysis of hybrid nanofluid as a coolant. *Procedia engineering*, 97, pp.1667-1675.
- [4]. Hayat, T. and Nadeem, S., 2017. Heat transfer enhancement with Ag–CuO/water hybrid nanofluid. *Results in physics*, 7, pp.2317-2324.
- [5]. Huang, D., Wu, Z. and Sunden, B., 2016. Effects of hybrid nanofluid mixture in plate heat exchangers. *Experimental Thermal and Fluid Science*, 72, pp.190-196.
- [6]. Rostami, M.N., Dinarvand, S. and Pop, I., 2018. Dual solutions for mixed convective stagnation-point flow of an aqueous silica–alumina hybrid nanofluid. *Chinese Journal of Physics*, 56(5), pp.2465-2478.
- [7]. Khashi'ie, N.S., Md Arifin, N. and Pop, I., 2020. Mixed convective stagnation point flow towards a vertical Riga plate in hybrid Cu-Al<sub>2</sub>O<sub>3</sub>/water nanofluid. *Mathematics*, 8(6), p.912.
- [8]. Cimpean, D.S., Sheremet, M.A. and Pop, I., 2020. Mixed convection of hybrid nanofluid in a porous trapezoidal chamber. *International Communications in Heat and Mass Transfer*, 116, p.104627.
- [9]. Albeshri, B.A.B., Islam, N., Bokhary, A.Y. and Pasha, A.A., 2021. Hydrodynamic Analysis of Laminar Mixed Convective Flow of Ag-TiO<sub>2</sub>-Water Hybrid Nanofluid in a Horizontal Annulus. *CFD Letters*, 13(7), pp.47-57.
- [10]. I-Rashed, A.A., 2022. Thermal management of lithium-ion batteries with simultaneous use of hybrid nanofluid and nano-enhanced phase change material: A numerical study. *Journal of Energy Storage*, 46, p.103730.
- [11]. Al-Rashed, A.A., 2022. Thermal management of lithium-ion batteries with simultaneous use of hybrid nanofluid and nano-enhanced phase change material: A numerical study. *Journal of Energy Storage*, 46, p.103730.
- [12]. Shoeibi, S., Kargarsharifabad, H., Rahbar, N., Ahmadi, G. and Safaei, M.R., 2022. Performance evaluation of a solar still using hybrid nanofluid glass cooling-CFD simulation and environmental analysis. *Sustainable Energy Technologies and Assessments*, 49, p.101728.
- [13]. Peng, R., He, X., Tang, X., Tong, J., Zhao, L. and Peng, X., 2022. An investigation into

the synergistic strengthening mechanism of ionic liquid and nanoparticles as a hybrid nanofluid in friction interface. *Tribology International*, 165, p.107298.

[14]. Vallejo, J.P., Żyła, G., Ansia, L., Fal, J., Traciak, J. and Lugo, L., 2022. Thermophysical, rheological and electrical properties of mono and hybrid TiB<sub>2</sub>/B<sub>4</sub>C nanofluids based on a propylene glycol: water mixture. *Powder Technology*, 395, pp.391-399.

[15]. Haq, R.U., Hamouch, Z., Hussain, S.T. and Mekkaoui, T., 2017. MHD mixed convection flow along a vertically heated sheet. *international journal of hydrogen energy*, 42(24), pp.15925-15932.

[16]. Oyelakin, I.S., Mondal, S. and Sibanda, P., 2017. Cattaneo–Christov nanofluid flow and heat transfer with variable properties over a vertical cone in a porous medium. *International Journal of Applied and Computational Mathematics*, 3(1), pp.1019-1034.

[17]. Reddy, P.R.K. and Raju, M.C., 2018. MHD free convective flow past a porous plate. *International journal of Pure and applied Mathematics*, 118(5), pp.507-529.

[18]. EL-Zahar, Essam R., Ahmed M. Rashad, and Laila F. Seddek. "The impact of sinusoidal surface temperature on the natural convective flow of a ferrofluid along a vertical plate." *Mathematics* 7.11 (2019): 1014.

[19]. Tlili, I., Sandeep, N., Reddy, M.G. and Nabwey, H.A., 2020. Effect of radiation on engine oil-TC<sub>4</sub>/NiCr mixture nanofluid flow over a revolving cone in mutable permeable medium. *Ain Shams Engineering Journal*, 11(4), pp.1255-1263.

[20]. Haritha, A., Devasena, Y., & Vishali, B. (2017). MHD heat and mass transfer of the unsteady flow of a Maxwell fluid over a stretching surface with Navier slip and convective boundary conditions. *Global Journal of Pure and Applied Mathematics*, 13(6), 2169-2179.

[21]. Madhu, M., Kishan, N., & Chamkha, A. J. (2017). Unsteady flow of a Maxwell nanofluid over a stretching surface in the presence of magnetohydrodynamic and thermal radiation effects. *Propulsion and Power research*, 6(1), 31-40.

[22]. Alsaedi, A., Muhammad, K., & Hayat, T. (2022). Numerical study of MHD hybrid nanofluid flow between two coaxial cylinders. *Alexandria Engineering Journal*, 61(11), 8355-8362.

[23]. Ahmad, S., Khan, M. N., Nadeem, S., Rehman, A., Ahmad, H., & Ali, R. (2021). Impact of Joule heating and multiple slips on a Maxwell nanofluid flow past a slendering surface. *Communications in Theoretical Physics*, 74(1), 015001.

[24]. Acharya, N. (2022). Buoyancy driven magnetohydrodynamic hybrid nanofluid flow within a circular enclosure fitted with fins. *International Communications in Heat and Mass Transfer*, 133, 105980.

- [25]. Neethu, T. S., Sabu, A. S., Mathew, A., Wakif, A., & Areekara, S. (2022). Multiple linear regression on bioconvective MHD hybrid nanofluid flow past an exponential stretching sheet with radiation and dissipation effects. *International Communications in Heat and Mass Transfer*, 135, 106115.
- [26]. Wahid, N. S., Arifin, N. M., Khashi'ie, N. S., Pop, I., Bachok, N., & Hafidzuddin, M. E. H. (2022). MHD mixed convection flow of a hybrid nanofluid past a permeable vertical flat plate with thermal radiation effect. *Alexandria Engineering Journal*, 61(4), 3323-3333.
- [27]. Algehyne, E. A., Alharbi, A. F., Saeed, A., Dawar, A., Ramzan, M., & Kumam, P. (2022). Analysis of the MHD partially ionized GO-Ag/water and GO-Ag/kerosene oil hybrid nanofluids flow over a stretching surface with Cattaneo–Christov double diffusion model: A comparative study. *International Communications in Heat and Mass Transfer*, 136, 106205.
- [28]. Mourad, A., Aissa, A., Abed, A. M., Toghraie, D., Akbari, O. A., Guedri, K., ...& Marzouki, R. (2023). MHD natural convection of Fe<sub>3</sub>O<sub>4</sub>-MWCNT/Water hybrid nanofluid filled in a porous annulus between a circular cylinder and Koch snowflake. *Alexandria Engineering Journal*, 65, 367- 382.
- [29]. Salmi, A., Madkhali, H. A., Nawaz, M., Alharbi, S. O., & Alqahtani, A. S. (2022). Numerical study on non-Fourier heat and mass transfer in partially ionized MHD Williamson hybrid nanofluid. *International Communications in Heat and Mass Transfer*, 133, 105967.
- [30]. Waqas, H., Farooq, U., Liu, D., Abid, M., Imran, M., & Muhammad, T. (2022). Heat transfer analysis of hybrid nanofluid flow with thermal radiation through a stretching sheet: A comparative study. *International Communications in Heat and Mass Transfer*, 138, 106303.
- [31]. Korei, Z., Benissaad, S., Berrahil, F., & Filali, A. (2022). MHD mixed convection and irreversibility analysis of hybrid nanofluids in a partially heated lid-driven cavity chamfered from the bottomside. *International Communications in Heat and Mass Transfer*, 132, 105895.
- [32]. Waini, Iskandar, Anuar Ishak, and Ioan Pop. "Symmetrical solutions of hybrid nanofluid stagnation-point flow in a porous medium." *International Communications in Heat and Mass Transfer* 130 (2022): 105804.
- [33]. Gangadhar, K., Subba Rao, M. V., Surekha, P., & Kannan, T. (2022). Shape effects on 3D MHD micropolar Au-MgO/blood hybrid nanofluid with Joule Heating. *International Journal of Ambient Energy*, 43(1), 8428-8437.
- [34]. Dawar, A., Wakif, A., Thumma, T., & Shah, N. A. (2022). Towards a new MHD non-homogeneous convective nanofluid flow model for simulating a rotating inclined thin layer of sodium alginate-based Iron oxide exposed to incident solar energy. *International Communications in Heat and Mass Transfer*, 130, 105800.

- [35]. Vajravelu, K. (2001). Viscous flow over a nonlinearly stretching sheet. *Applied mathematics and computation*, 124(3), 281-288.
- [36]. Tsou, F. K., Sparrow, E. M., & Goldstein, R. J. (1967). Flow and heat transfer in the boundary layer on a continuous moving surface. *International Journal of Heat and Mass Transfer*, 10(2), 219-235.
- [37]. Fang, T., & Yao, S. (2011). Viscous swirling flow over a stretching cylinder. *Chinese Physics Letters*, 28(11), 114702.
- [38]. Sprague, M. A., & Weidman, P. D. (2010). Three-dimensional flow induced by the torsional motion of a cylinder. *Fluid Dynamics Research*, 43(1), 015501.
- [39]. Seddeek, M. A., & Abdelmeguid, M. S. (2006). Effects of radiation and thermal diffusivity on heat transfer over a stretching surface with variable heat flux. *Physics Letters A*, 348(3-6), 172-179.
- [40]. Hassan, H. S. (2015). Symmetry analysis for MHD viscous flow and heat transfer over a stretching sheet. *Applied Mathematics*, 6(01), 78.
- [41]. Qi, D., Cao, Z., & Ziener, U. (2014). Recent advances in the preparation of hybrid nanoparticles in miniemulsions. *Advances in colloid and interface science*, 211, 47-62.
- [42]. Aaron, J. S., Oh, J., Larson, T. A., Kumar, S., Milner, T. E., & Sokolov, K. V. (2006). Increased optical contrast in imaging of epidermal growth factor receptor using magnetically actuated hybrid gold/iron oxide nanoparticles. *Optics express*, 14(26), 12930-12943.
- [43]. Devarajan, M., Parasumanna Krishnamurthy, N., Balasubramanian, M., Ramani, B., Wongwises, S., Abd El-Naby, K., & Sathyamurthy, R. (2018). Thermophysical properties of CNT and CNT/Al<sub>2</sub>O<sub>3</sub> hybrid nanofluid. *Micro & Nano Letters*, 13(5), 617-621.
- [44]. Esfe, M. H., Arani, A. A. A., Madadi, M. R., & Alirezaie, A. (2018). A study on rheological characteristics of hybrid nano-lubricants containing MWCNT-TiO<sub>2</sub> nanoparticles. *Journal of Molecular Liquids*, 260, 229-236
- [45]. Yaseen, M., Rawat, S. K., Shafiq, A., Kumar, M., & Nonlaopon, K. (2022). Analysis of heat transfer of mono and hybrid nanofluid flow between two parallel plates in a Darcy porous medium with thermal radiation and heat generation/absorption. *Symmetry*, 14(9), 1943.
- [46]. Bayones, F. S., Jamshed, W., Elhag, S. H., & Rabea Eid, M. (2022). Computational Galerkin finite element method for thermal hydrogen energy utilization of first grade viscoelastic hybrid nanofluid flowing inside PTSC in solar powered ship applications. *Energy & Environment*, 0958305X221081463.
- [47]. Nalivela, N. R., Vempati, S. R., Ravindra Reddy, B., & Dharmendar Reddy, Y. (2022). Viscous dissipation and thermal radiation impact on MHD mass transfer natural convective

flow over a stretching sheet. *Proceedings of the Institution of Mechanical Engineers, Part E: Journal of Process Mechanical Engineering*, 09544089221081339.

[48]. Punith Gowda, R. J., Naveen Kumar, R., Jyothi, A. M., Prasannakumara, B. C., & Nisar, K. S. (2021). KKL correlation for simulation of nanofluid flow over a stretching sheet considering magnetic dipole and chemical reaction. *ZAMM-Journal of Applied Mathematics and Mechanics/Zeitschrift für Angewandte Mathematik und Mechanik*, 101(11), e202000372.

[49]. Eid, M. R., & Nafe, M. A. (2022). Thermal conductivity variation and heat generation effects on magneto-hybrid nanofluid flow in a porous medium with slip condition. *Waves in Random and Complex Media*, 32(3), 1103-1127.

[50]. Aly, A. M., & Raizah, Z. A. S. (2019). Mixed convection in an inclined nanofluid filled-cavity saturated with a partially layered porous medium. *Journal of Thermal Science and Engineering Applications*, 11(4).

[51]. Aly. E. H. and I. Pop. (2020). MHD áow and heat transfer near stagnation point over a stretching/shrinking surface with partial slip and viscous dissipation: Hybrid nanoáuid versus nanoáuid. *Powder Technology*. 365 ,467-563.

[52]. Salawu, S. O., Fatunmbi, E. O., & Okoya, S. S. (2021). MHD heat and mass transport of Maxwell Arrhenius kinetic nanofluid flow over stretching surface with nonlinear variable properties. *Results in Chemistry*, 3, 100125.

[53]. Adigun, J. A., Adeniyani, A., & Abiala, I. O. (2021). Stagnation point MHD slip-flow of viscoelastic nanomaterial over a stretched inclined cylindrical surface in a porous medium with dual stratification. *International Communications in Heat and Mass Transfer*, 126, 105479.

[54]. Hamzah, H. K., Ali, F. H., & Hatami, M. (2022). MHD mixed convection and entropy generation of CNT-water nanofluid in a wavy lid-driven porous enclosure at different boundary conditions. *Scientific Reports*, 12(1), 2881.

[55]. Labib, M. N., Nine, M. J., Afrianto, H., Chung, H., & Jeong, H. (2013). Numerical investigation on effect of base fluids and hybrid nanofluid in forced convective heat transfer. *International Journal of Thermal Sciences*, 71, 163-171.

[56]. Lund, L. A., Omar, Z., Khan, I., & Sherif, E. S. M. (2020). Dual solutions and stability analysis of a hybrid nanofluid over a stretching/shrinking sheet executing MHD flow. *Symmetry*, 12(2), 276.

[57]. Sreedevi, P., Sudarsana Reddy, P., & Chamkha, A. (2020). Heat and mass transfer analysis of unsteady hybrid nanofluid flow over a stretching sheet with thermal radiation. *SN Applied Sciences*, 2(7), 1222.

[58]. Nabwey, H. A., & Mahdy, A. (2021). Transient flow of micropolar dusty hybrid

nanofluid loaded with Fe<sub>3</sub>O<sub>4</sub>-Ag nanoparticles through a porous stretching sheet. *Results in Physics*, 21, 103777.

[59]. Ajibade, A. O., & Umar, A. M. (2020). Effects of viscous dissipation and boundary wall thickness on steady natural convection Couette flow with variable viscosity and thermal conductivity. *International Journal of Thermofluids*, 7, 100052.

[60]. Huminic, G., Huminic, A., Dumitrache, F., Fleacă, C., & Morjan, I. (2020). Study of the thermal conductivity of hybrid nanofluids: Recent research and experimental study. *Powder technology*, 367, 347-357.

[61]. Hussain, Z. (2020). Heat transfer through temperature dependent viscosity hybrid nanofluid subject to homogeneous-heterogeneous reactions and melting condition: A comparative study. *Physica Scripta*, 96(1), 015210.

[62]. Jana, S., Salehi-Khojin, A., & Zhong, W. H. (2007). Enhancement of fluid thermal conductivity by the addition of single and hybrid nano-additives. *Thermochimica acta*, 462(1-2), 45-55.

[63]. B. Johnson, A., & B. I, O. (2023). Impact of radiation and heat generation/absorption in a Walters' B fluid through a porous medium with thermal and thermo diffusion in the presence of chemical reaction. *International Journal of Modelling and Simulation*, 43(2), 87-100.

[64]. Roy, N. C., & Pop, I. (2022). Heat and mass transfer of a hybrid nanofluid flow with binary chemical reaction over a permeable shrinking surface. *Chinese Journal of Physics*, 76, 283-298.

[65]. Sulochana. C. S., Aparna.R. and Sandeep.N. (2022). Impact of linear/nonlinear radiation on incessantly moving thin needle in MHD quiescent Al-Cu/methanol hybrid nanoáuid. *International Journal of Ambient Energy*. 43(1), 2694-2700

[66]. Hosseinzadeh, K., Gholinia, M., Jafari, B., Ghanbarpour, A., Olfian, H., & Ganji, D. D. (2019). Nonlinear thermal radiation and chemical reaction effects on Maxwell fluid flow with convectively heated plate in a porous medium. *Heat Transfer—Asian Research*, 48(2), 744-759.

[67]. Rahimi, J., Ganji, D. D., Khaki, M., & Hosseinzadeh, K. (2017). Solution of boundary layer flow of an Eyring-Powell non-Newtonian fluid over a linear stretching sheet by collocation method. *Alexandria Engineering Journal*, 56(4), 621-627.

[68]. Kempannagari, A. K., Buruju, R. R., Naramgari, S., & Vangala, S. (2020). Effect of Joule heating on MHD non-Newtonian fluid flow past an exponentially stretching curved surface. *Heat Transfer*, 49(6), 3575-3592.

[69]. Singh, J. K., & Seth, G. S. (2022). Heat and mass transport performance of MHD elastico-



viscous fluid flow over a vertically oriented magnetized surface with magnetic and thermo diffusions. *Heat Transfer*, 51(2), 2258-2278.

[70]. Abu Bakar, S., Md Arifin, N., Khashi'ie, N. S., & Bachok, N. (2021). Hybrid nanofluid flow over a permeable shrinking sheet embedded in a porous medium with radiation and slip impacts. *Mathematics*, 9(8), 878.

[71]. Khan, M., Sarfraz, M., Ahmed, A., & Fatima, U. U. K. (2022). Insight into the addition of multi-walled carbon nanotubes to dynamics of water conveying single surface carbon nanotubes due to torsional motion of cylinder subject to Lorentz force and joule heating. *International Journal of Modern Physics B*, 36(22), 2250138.